CONFIDENTIAL

Copy
RM L50G14b

NACA

RESEARCH MEMORANDUM

EXPERIMENTAL DETERMINATION OF EFFECT OF STRUCTURAL RIGIDITY ON ROLLING EFFECTIVENESS OF SOME STRAIGHT AND SWEPT WINGS AT MACH NUMBERS FROM 0.7 TO 1.7

By H. Kurt Strass, E. M. Fields,
and Paul E. Purser

Langley Aeronautical Laboratory
Langley Air Force Base, Va.

NATIONAL ADVISORY COMMITTEE
FOR AERONAUTICS

WASHINGTON

October 4, 1950

CONFIDENTIAL

Classification cancelled (or changed to Unclassified)

By Authority of NASA Tech Pub Announcement
(OFFICER AUTHORIZED TO CHANGE) 89 8 Sept 05

By .....

.....
(GRADE OF OFFICER MAKING CHANGE)

11 Apr 61
DATE

NATIONAL ADVISORY COMMITTEE FOR AERONAUTICS

RESEARCH MEMORANDUM

EXPERIMENTAL DETERMINATION OF EFFECT OF STRUCTURAL RIGIDITY ON ROLLING EFFECTIVENESS OF SOME STRAIGHT AND SWEPT WINGS AT MACH NUMBERS FROM 0.7 TO 1.7

By H. Kurt Strass, E. M. Fields,
and Paul E. Purser

SUMMARY

The effect of varying the wing structural rigidity on the control effectiveness of 0.2-chord, plain, faired, full-span ailerons on untapered wing plan forms having 0° and 45° sweep and aspect ratio of 3.7 has been investigated by the Langley Pilotless Aircraft Research Division by utilizing rocket-propelled test vehicles.

The results of the tests indicate no radical differences between straight and swept wings in the changes in rolling effectiveness due to changes in structural rigidity.

The test results compare favorably with results obtained by use of existing methods of estimating the effects of structural rigidity on rolling effectiveness for unswept wings (NACA Rep. 799 and NACA TN 1890) at subsonic and supersonic speeds. As an illustration of the use of the experimental data, they have been analyzed by the method of NACA Rep. 799 to provide approximate twisting-moment coefficients for an extension of that method to transonic speeds and swept wings.

INTRODUCTION

The problem of estimating the rolling power of controls on flexible wings continually faces the designer. Relatively simple methods for making such estimations for unswept wings at both subsonic and supersonic speeds have been advanced in references 1 to 6. The present investigation was undertaken to provide a check on these methods in the speed range where existing aerodynamic theories are applicable and to obtain data at transonic speeds in order to offer some guide to the designers now interested in aircraft which are to fly near a Mach number of 1.

All of the wings tested were untapered with an aspect ratio of 3.7 and employed full-span plain ailerons. Information was obtained for six values of structural rigidity on unswept wings and five values of structural rigidity on wings swept back 45°. All of the foregoing wings employed the NACA 65A009 airfoil section parallel to the model center line. In addition, two values of structural rigidity were investigated for unswept wings which employed the NACA 65A003 airfoil section. The structural rigidity, referred to as "torsional rigidity" throughout this paper, is the usual torsional rigidity for unswept wings. For swept wings, however, the torsional rigidity used herein was derived from torques applied and twists measured in planes parallel to the model center line and thus includes both bending and torsional stiffness as usually defined. All of the data were obtained in free flight from rocket-propelled test vehicles by means of the technique described in reference 7, which permits the evaluation of the rolling power of wing-aileron configurations continuously over a Mach number range of approximately 0.7 to 1.7.

SYMBOLS

A	aspect ratio, 3.7 (b^2/S)
b	diameter of circle swept by wing tips (with regard to rolling characteristics, this diameter is considered to be the effective span of three-fin models), 2.18 feet
S	area of two wing panels measured to fuselage center line, 1.29 square feet
c	wing chord parallel to model center line, 0.59 foot
M	Mach number
m	concentrated couple, applied near wing tip in a plane parallel to free stream and normal to wing chord plane, foot-pound
P	static pressure, pounds per square foot
q	dynamic pressure, pounds per square foot
p	rolling velocity, radians per second
V	flight-path velocity, feet per second
pb/2V	wing-tip helix angle, radians

c_m section pitching-moment coefficient $\left(\frac{\text{Section pitching moment}}{qc}\right)$

$\frac{dc_m/d\delta}{d\alpha/d\delta}$ section twisting-moment parameter for constant lift

$dc_m/d\delta$ rate of change of section pitching-moment coefficient with aileron angle per radian

$d\alpha/d\delta$ rate of change of wing angle of attack with aileron angle as obtained for constant lift at section

δ_a deflection of each aileron measured in plane perpendicular to chord plane and parallel to model center line (average for three wings), degrees

i_w average wing incidence for three wings measured in plane of δ_a, positive when tending to produce clockwise roll as seen from rear, degrees

λ ratio of tip chord to root chord at model center line

Λ angle of sweep, degrees

θ angle of twist, produced by m, at any section along wing span in a plane parallel to free stream and normal to wing-chord plane, radians

$l/m\theta_r$ wing-torsional-stiffness parameter, measured at exposed aileron midspan parallel to model center line, radians per foot-pound (θ/m)

ρ mass density of air, slugs per cubic foot

γ ratio for specific heats for air, 1.40

τ derived constant for wing and aileron (see reference 1), 0.585

φ fraction of rigid-wing rolling effectiveness retained by flexible wing

Subscripts:

a altitude

o sea level

r	reference station (middle of exposed aileron span)
R	rigid
F	flexible

MODELS AND TECHNIQUE

The test vehicles used in the present investigation are described in the photograph presented as figure 1 and in the sketch of figure 2. The exposed wing area was 1.56 square feet, the area of two wings taken to the center line of the fuselage was 1.29 square feet, and the aspect ratio A was 3.7. The ailerons were of 0.2 chord and simulated sealed, faired ailerons in that there was no surface discontinuity at the aileron hinge axis. The airfoil section parallel to the model center line for all models was either the NACA 65A009 or the NACA 65A003.

The test wings are described in figures 3 and 4. The construction shown is typical for the 9-percent-thick wings that employed metal inlays for stiffness. The torsional rigidity of the 9-percent wings was generally varied by varying the thickness and material of the inlay; however, in the case of the weakest wings in the series, the metal inlay was not used and the stiffness was varied by the choice of the wood of which the wings were constructed. The stiffness of the 3-percent wings was varied by constructing the wings of solid aluminum alloy or cold-rolled steel.

The torsional-stiffness parameters of all the test wings were obtained by applying a known couple at the wing tip and measuring the resulting twist along the span. The couple was applied and the twist was measured in planes parallel to the free stream and normal to the wing chord plane. The variation of the torsional-stiffness parameter $1/m\theta$ with spanwise location was linear with spanwise distance out from the side of the body for all the test wings. Thus the stiffness for any spanwise station may be obtained from the value given for the reference station. A more complete description of the types of construction of the various test wings is given in table I.

The flight tests were made at the Pilotless Aircraft Research Station, Wallops Island, Va. The test vehicles were propelled by a two-stage rocket-propulsion system to a Mach number of about 1.7. During a 10-second period of coasting flight following rocket-motor burnout, time histories of the rolling velocity were obtained with special radio equipment and the flight-path velocity was obtained by the use of CW Doppler radar. These data, in conjunction with atmospheric data obtained with radiosondes, permit the evaluation of the

aileron rolling effectiveness in terms of the parameter $pb/2V$ as a function of Mach number. The Reynolds number for the tests varied from approximately 3.0×10^6 at $M = 0.7$ to 7.0×10^6 at $M = 1.7$. Reference 7 gives a more complete description of the flight testing technique.

ACCURACY AND CORRECTIONS

Estimation of the experimental error depends upon the evaluation of two distinct factors: The random scatter inherent in the recording and reduction of the data and the systematic error caused by the limitations in model measuring accuracy. Based upon previous experience, these factors are estimated to be within the following limits:

	Subsonic			Supersonic		
	Random	Systematic	Total	Random	Systematic	Total
$pb/2V$	±0.0020	±0.0035	±0.0055	±0.0010	±0.0015	±0.0025
M	±0.01	-------	±0.01	±0.01	-------	±0.01

The accuracy of Δi_w (departure from measured values) is $\pm 0.05^\circ$; and that for $\Delta \delta_a$ (departure from measured values) is $\pm 0.1^\circ$.

Because close tolerances on models of the type used in this investigation are extremely difficult to maintain, slight variations from the nominal values of $i_w = 0^\circ$ and $\delta_a = 5^\circ$ are permitted. Since a method of measuring the important parameters of the test vehicles to close limits was used, the assumption was made that such discrepancies would be of small enough order of magnitude to allow linear correction of the data to the nominal values. The data were corrected for incidence by use of the following equation which was derived from strip theory for rigid wings:

$$\frac{pb}{2V} = \frac{2i_w}{57.3}\left(\frac{1 + 2\lambda}{1 + 3\lambda}\right) = 0.0262 i_w$$

The validity of this correction is demonstrated in figure 5 where the experimental values of $pb/2V$ obtained for wings similar to those used in the present investigation are compared with the calculated values. It will be noted that the agreement is good throughout most of the speed range, although the variation of $pb/2V$ with Mach number for the unswept wings shows a fluctuation between $M = 0.88$ and $M = 1.05$. This sudden

change in rate of roll has been observed previously and is discussed in reference 8, which presents data that indicate that the magnitude of the fluctuation is affected by airfoil shape, thickness ratio, and wing sweep.

The corrections for aileron deflection were made by reducing the data to $\frac{pb/2V}{\delta_a}$ and then multiplying by the nominal δ_a value of 5°. All the data presented have been corrected to nominal incidence and aileron-setting values of 0° and 5°, respectively. The actual measured values for the models tested are presented in table I in order to show the magnitude of such corrections.

No attempt was made to correct for the effect of the test-vehicle moment of inertia about the roll axis on the measured variation of $pb/2V$ with Mach number since the method of analysis suggested in reference 7 indicated that the magnitude of the correction is small enough not to affect the conclusions drawn from these data.

RESULTS AND DISCUSSION

Torsional Rigidity

The term "torsional rigidity" as used in the following discussion is based on torques applied and twists measured in planes parallel to the fuselage center line. The values for swept wings therefore include both the torsional and bending rigidity as usually defined in planes parallel and perpendicular to the main spar, torsion box, or other primary wing structure.

Experimental Data

The data obtained during the present investigation are presented in figures 6 to 8 as curves of $pb/2V$ against Mach number. The static pressure existing during each flight is also shown on the figures as P_a/P_o, the ratio of static pressure at the altitude of the test to standard sea-level static pressure (2116 lbs/sq ft). The data are presented as separate plots for duplicate models of each configuration in order to show the agreement obtained with supposedly identical models. Figure 6 presents the data for the unswept 9-percent-thick wings; figure 7, the 45° sweptback 9-percent wings; and figure 8, the unswept 3-percent wings.

Because different atmospheric conditions prevailed for the various tests and because the data were obtained over an altitude range of

approximately 10,000 feet, it was necessary to correct all of the rolling-effectiveness data to standard sea-level conditions to provide an adequate basis for comparison. This correction was made by plotting $pb/2V$ as a function of the torsional-stiffness criterion $1/m_{\theta_r}$ at constant Mach number and extrapolating to $\frac{1}{m_{\dot{\theta}_r}} = 0$ by use of the method of least squares to obtain consistent values of $pb/2V$ for the infinitely rigid wing. It was assumed that the rolling effectiveness of a rigid wing would be unaffected by a change in altitude and that the loss in rolling effectiveness due to wing twisting at constant Mach number would be proportional to the static pressure. The assumed relationships can be stated as follows:

$$m = Kq = K \frac{\gamma}{2} PM^2 \tag{1}$$

where K is an arbitrary constant and m is the aerodynamic twisting moment.

At the same Mach number:

$$\frac{m_1}{m_2} = \frac{P_1}{P_2} \tag{2}$$

$$\left[\left(\frac{pb}{2V}\right)_R\right]_a = \left[\left(\frac{pb}{2V}\right)_R\right]_o \tag{3}$$

$$\frac{\left[(pb/2V)_R - (pb/2V)_F\right]_a}{\left[(pb/2V)_R - (pb/2V)_F\right]_o} = \frac{m_a}{m_o} = \frac{P_a}{P_o} \tag{4}$$

$$\left(\frac{pb}{2V}\right)_{F_o} = \left(\frac{pb}{2V}\right)_R - \frac{P_o}{P_a}\left[\left(\frac{pb}{2V}\right)_R - \left(\frac{pb}{2V}\right)_F\right]_a$$

The corrected data are presented in figure 9 and show the effect of decreasing wing torsional rigidity on the variation of rolling effectiveness with Mach number at sea level. Averaged data are presented for the cases where duplicate test vehicles were flown. It should be noted that the models with the most flexible wings in both the swept and unswept series would roll against the applied control rolling moment throughout the entire supersonic speed range tested.

Figure 10 presents the data shown in figure 9 cross-plotted and expressed in ratio form to show the relative loss in control effectiveness with decreasing torsional rigidity at constant values of Mach number.

Comparison of Theory and Experiment

Because of the linear nature of the curves in figure 10, the information presented therein can be given by a plot of the slopes of the curves $\frac{d\varphi}{d\left(1/m_{\theta_r}\right)}$ for each angle of sweep and airfoil section against Mach number. These curves are presented in figure 11 together with the corresponding theoretical curves for the unswept wing. The subsonic theoretical values were calculated by use of the method described in reference 1 and the supersonic values according to references 2 to 4. The second-order correction for trailing-edge angle from reference 2 was replaced by the corresponding third-order factor from reference 3. This procedure was recommended by the authors of references 2 and 3.

The data shown in figure 11 indicate little effect of airfoil section on the rate of change of loss in relative rolling effectiveness with change in torsional rigidity $\frac{d\varphi}{d\left(1/m_{\theta_r}\right)}$. The values calculated from theory show an effect of airfoil section (trailing-edge angle) at supersonic speeds, but the differences between the experimental and theoretical values are relatively small, 5 to 10 percent at $M \approx 1.5$. The experimental data also indicate that the effects of sweep on the value of $\frac{d\varphi}{d\left(1/m_{\theta_r}\right)}$ are not great. The effect of 45° of sweepback on $\frac{d\varphi}{d\left(1/m_{\theta_r}\right)}$ varies from zero at $M \approx 0.7$ to a 20-percent reduction at $M \approx 1.5$.

Figure 12 demonstrates how the experimentally determined variation of $pb/2V$ against Mach number compares with that of theory for selected values of torsional rigidity for the unswept NACA 65A009 wings. A similar comparison is presented for the NACA 65A003 wings in figure 13. A lifting-surface-theory correction from reference 5 was applied to the subsonic theoretical values for the rigid wings. This corrected rigid-wing value was then used in the computation of the flexible-wing rolling effectiveness. The generally good agreement between theory and experiment is encouraging in that it shows that the theory predicts equally well both the control effectiveness for the rigid wing and the loss due to flexibility.

Transonic Rolling Performance

The agreement of the experimental data with estimates based on references 1 to 5 indicates that losses in aileron performance can be predicted at subsonic and supersonic speeds with satisfactory accuracy for most purposes. This statement implies, of course, that in regions where the aerodynamic coefficients are known the effects of structural flexibility can be satisfactorily estimated. It should be possible, therefore, to utilize the observed losses in rolling performance and the known structural properties of the test wings to determine the aerodynamic twisting moments upon which the losses depend. This procedure should then provide useful data for the transonic speed range where the greatest lack of such data now exists.

As an example, the method of reference 1 has been used to obtain twisting moments from the present data because of the ease and rapidity with which this method may be applied.

Equation (1) of reference 1 was rewritten in the form

$$\frac{dc_m/d\delta}{d\alpha/d\delta} = \frac{1}{\tau}\frac{2A^2}{b^3}\frac{m_{\theta_r}}{q}(1 - \varphi) \qquad (6)$$

in order to obtain effective values for $\frac{dc_m/d\delta}{d\alpha/d\delta}$ which are considered proportional to the twisting moments acting on the wing. The compressibility factor $\frac{1}{\sqrt{1 - M^2}}$ has been omitted from equation (6) since its use was recommended in reference 1 only where data at the Mach number of interest were not available. The values of A, b, and m_{θ_r} are the aspect ratio, span, and stiffness of the test wings. The value of q is the dynamic pressure at sea level and values of φ, the rolling-loss ratio at sea level, were obtained from figure 10. The value τ is a derived geometric and aerodynamic constant for the test wings and was obtained by a small extrapolation from the charts of reference 1.

Values of $\frac{dc_m/d\delta}{d\alpha/d\delta}$ determined from the experimental data by use of equation (6) are presented in figure 14 for the Mach number range from 0.7 to 1.6. Also shown in figure 14 are values of $\frac{dc_m/d\delta}{d\alpha/d\delta}$ calculated from linear theory to indicate the agreement of theory and experiment in the Mach number range where the theory is considered applicable.

The data in figure 14 indicate that in the transonic range a reduction in wing thickness decreased the abruptness of the variation with

Mach number of $\frac{dc_m/d\delta}{d\alpha/d\delta}$ and sweeping the wing back 45° reduced the twisting moments by about 20 percent.

The agreement of these pitching-moment data with other experimental data (reference 9, for instance) is about as good as the agreement with the theoretical values in the range where the linear theory is applicable. This fact indicates, therefore, that obtaining twisting moments from experimental rolling-loss data is a promising procedure and should be pursued further in order to investigate more fully the effects of such variables as airfoil section and sweep.

CONCLUSIONS

An investigation of the effect of structural rigidity on the control effectiveness of 0.2-chord, plain, faired, full-span ailerons on untapered wing plan forms having 0° and 45° sweep and aspect ratio 3.7 gave the following conclusions:

1. No radical differences existed between the rate of change of relative rolling effectiveness with changes in structural rigidity for the straight and swept wings tested.

2. For unswept wings the existing methods and aerodynamic theories for estimating the loss in control effectiveness due to wing twisting are probably satisfactory for most purposes for both subsonic and supersonic speeds with the exception of the Mach number range between 0.9 and 1.2.

3. For swept wings and for straight wings at transonic speeds, twisting moments may be evaluated from these test data for use with existing methods of estimating the loss in rolling effectiveness due to wing twist.

Langley Aeronautical Laboratory
National Advisory Committee for Aeronautics
Langley Air Force Base, Va.

REFERENCES

1. Pearson, Henry A., and Aiken, William S., Jr.: Charts for the Determination of Wing Torsional Stiffness Required for Specified Rolling Characteristics or Aileron Reversal Speed. NACA Rep. 799, 1944.

2. Tucker, Warren A., and Nelson, Robert L.: The Flexible Rectangular Wing in Roll at Supersonic Flight Speeds. NACA TN 1769, 1948.

3. Tucker, Warren A., and Nelson, Robert L.: Theoretical Characteristics in Supersonic Flow of Constant-Chord Partial-Span Control Surfaces on Rectangular Wings Having Finite Thickness. NACA TN 1708, 1948.

4. Tucker, Warren A., and Nelson, Robert L.: The Effect of Torsional Flexibility on the Rolling Characteristics at Supersonic Speeds of Tapered Unswept Wings. NACA TN 1890, 1949.

5. Swanson, Robert S., and Priddy, E. LaVerne: Lifting-Surface-Theory Values of the Damping in Roll and of the Parameter Used in Estimating Aileron Stick Forces. NACA ARR L5F23, 1945.

6. Langley Research Staff (Compiled by Thomas A. Toll): Summary of Lateral-Control Research. NACA Rep. 868, 1947.

7. Sandahl, Carl A., and Marino, Alfred A.: Free-Flight Investigation of Control Effectiveness of Full-Span 0.2-Chord Plain Ailerons at High Subsonic, Transonic, and Supersonic Speeds to Determine Some Effects of Section Thickness and Wing Sweepback. NACA RM L7D02, 1947.

8. Stone, David G.: Wing-Dropping Characteristics of Some Straight and Swept Wings at Transonic Speeds as Determined with Rocket-Powered Models. NACA RM L50C01, 1950.

9. Luoma, Arvo A.: An Investigation of a High-Aspect-Ratio Wing Having 0.20-Chord Plain Ailerons in the Langley 8-Foot High-Speed Tunnel. NACA RM L6H28d, 1946.

TABLE I

DESCRIPTION OF INDIVIDUAL TEST MODELS

$1/m_{\theta_r}$	Λ (deg)	NACA airfoil section	Model	i_w (deg)	δ_a (deg)	Type of construction
1.7×10^{-4}	0	65A009	1	-0.20	5.6	0.020-in. steel inlay, spruce core stock
			2	.07	5.1	
			3	.04	5.7	
2.6	0	65A009	1	-.04	4.9	0.010-in. steel inlay, spruce core stock
			2	-.08	4.9	
4.1	0	65A009	1	-.07	4.8	0.016-in. aluminum inlay, spruce core stock
9.6	0	65A009	1	0	4.9	Solid laminated beech
			2	-.09	5.0	
15.0	0	65A009	1	-.06	5.5	Solid laminated white pine
15.9	0	65A009	1	-.07	5.2	Solid laminated white pine
3.5	45	65A009	1	-.20	5.3	0.020-in. steel inlay, spruce core stock
			2	-.20	5.3	
4.5	45	65A009	1	.06	4.7	0.010-in. steel inlay, spruce core stock
6.5	45	65A009	1	-.03	5.2	0.016-in. aluminum inlay spruce core stock
			2	-.11	5.1	
12.4	45	65A009	1	.05	5.3	Solid laminated beech
23.7	45	65A009	1	.18	4.6	Solid laminated white pine
			2	.17	5.0	
4.7	0	65A003	1	-.24	5.5	Solid steel
14.7	0	65A003	1	-.06	4.9	Solid aluminum alloy

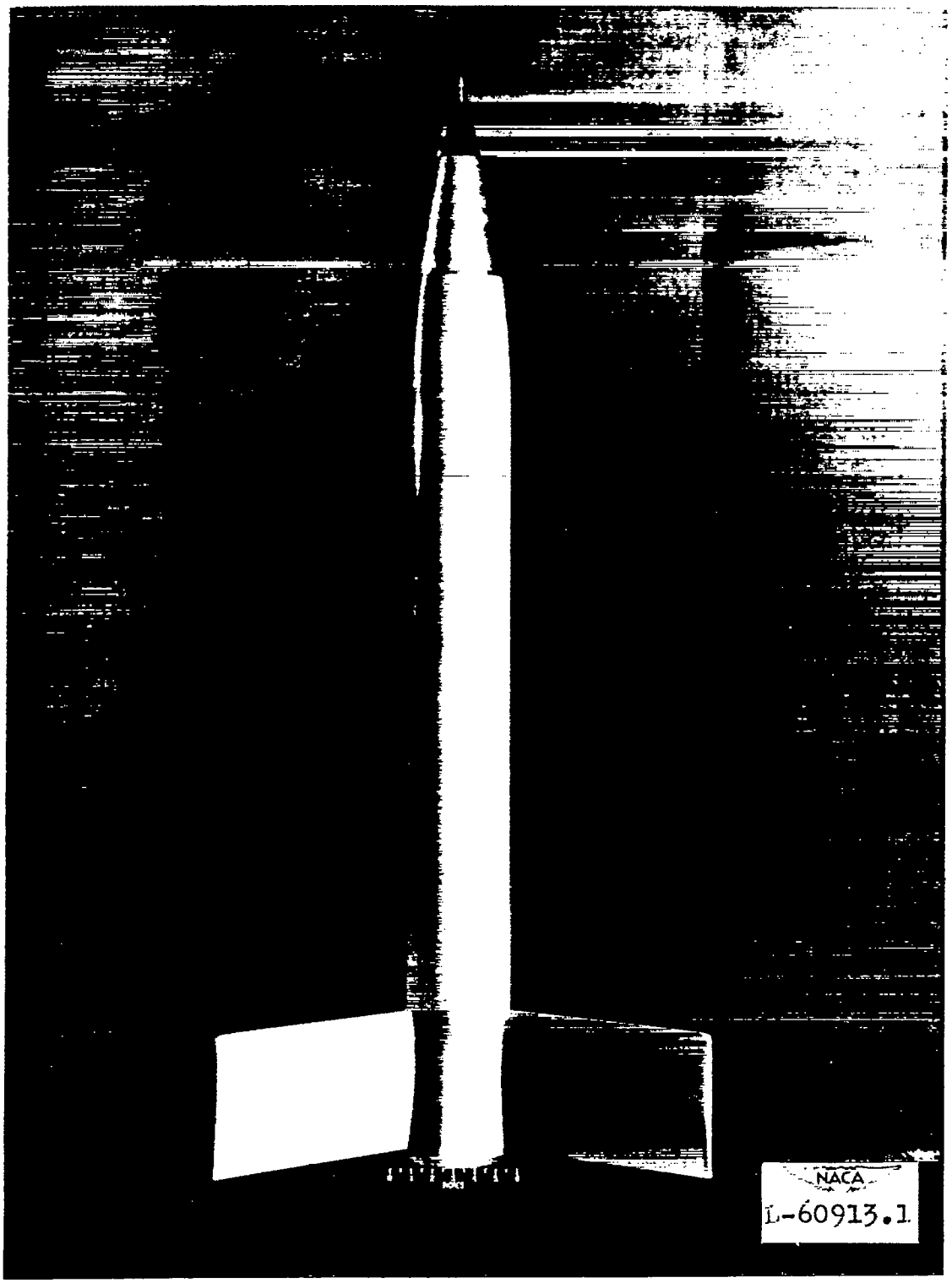

Figure 1.- Typical test model.

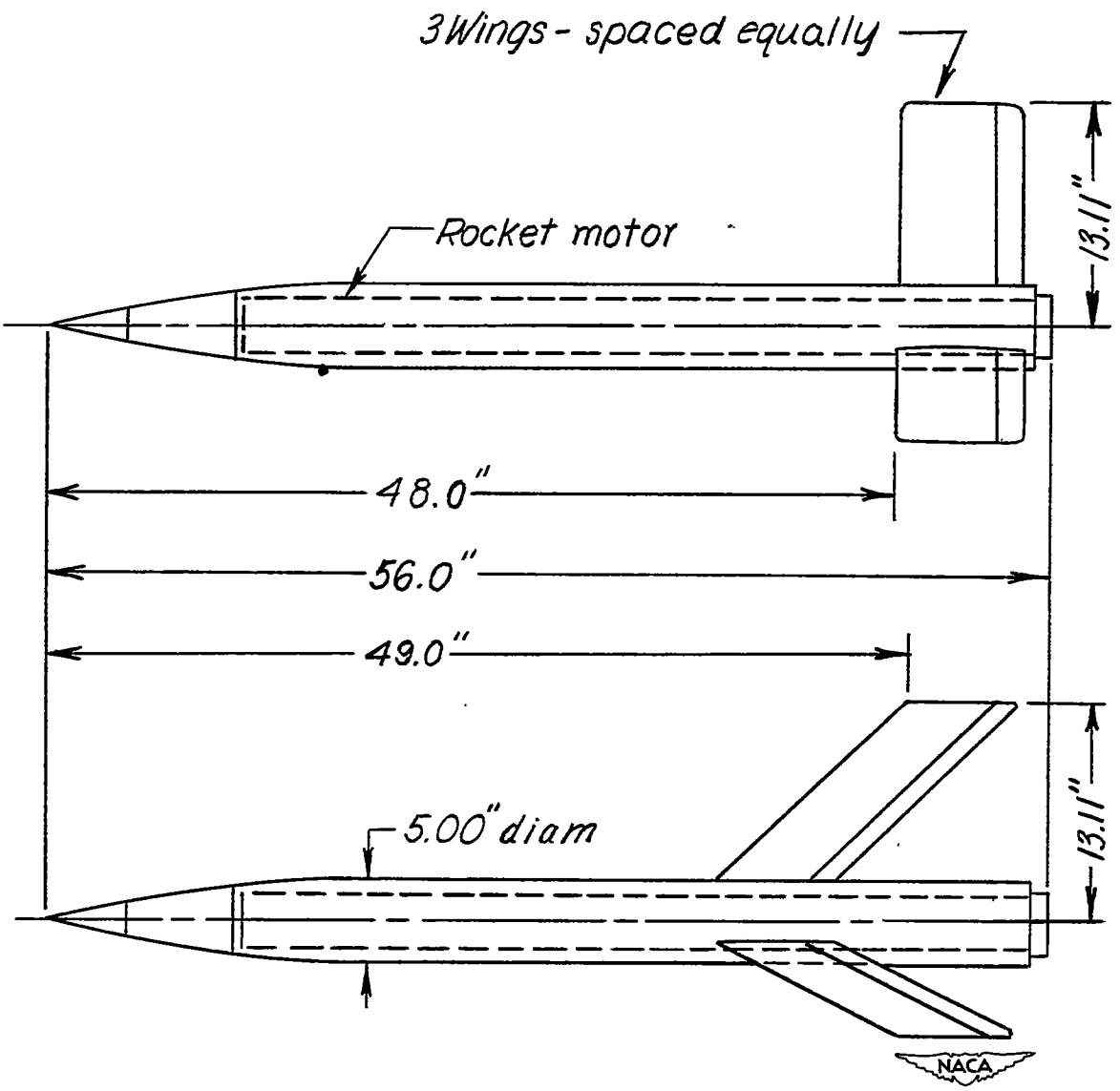

Figure 2.- Sketch of vehicle showing location of test wings and the geometric characteristics of models.

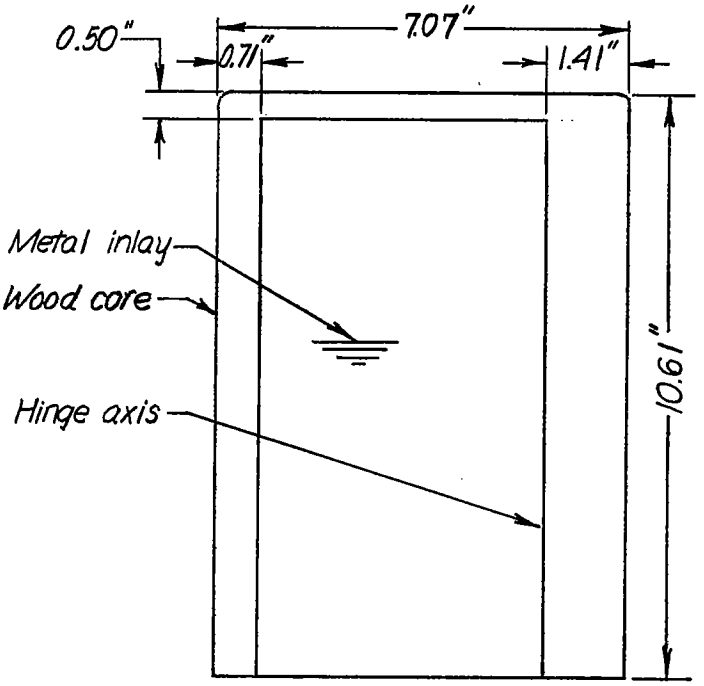

(a) Exposed wing panel.

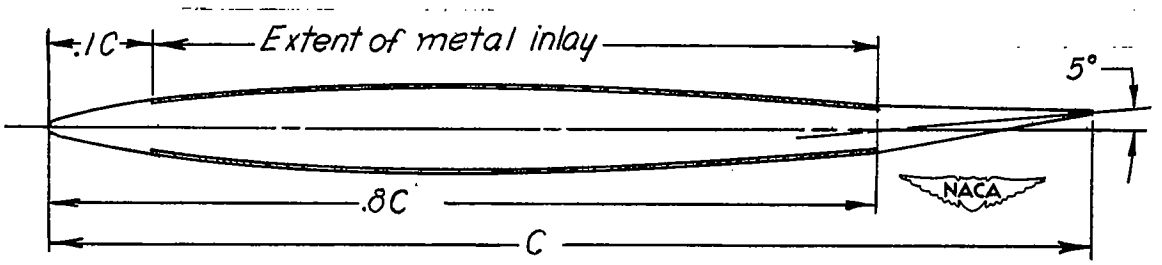

(b) Typical section.

Figure 3.- Description of unswept test wings.

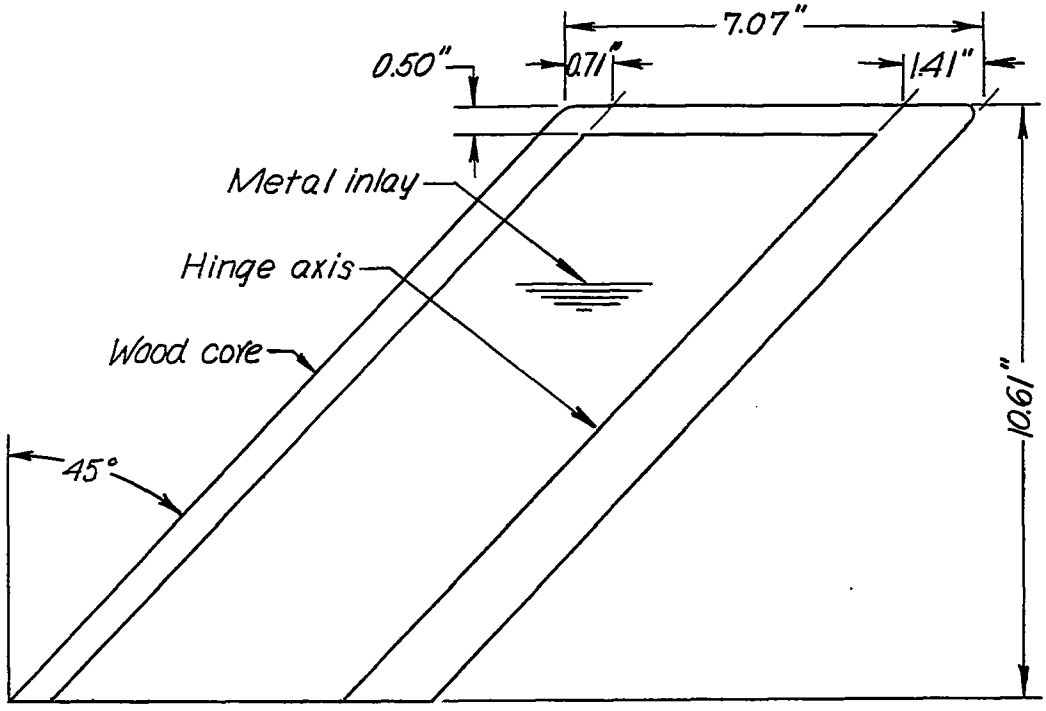

(a) Exposed wing panel.

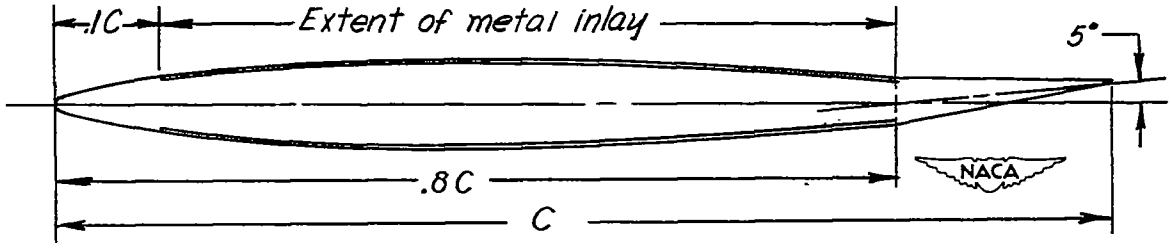

(b) Typical section.

Figure 4.- Description of swept test wings.

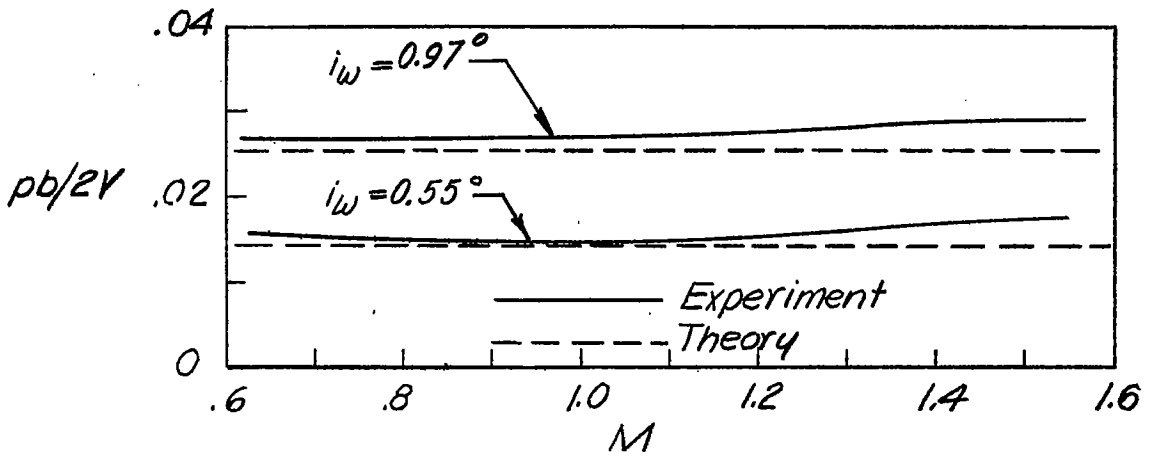

(a) $\Lambda = 45°$; $\frac{1}{m_{\theta_r}} = 3.5 \times 10^{-4}$.

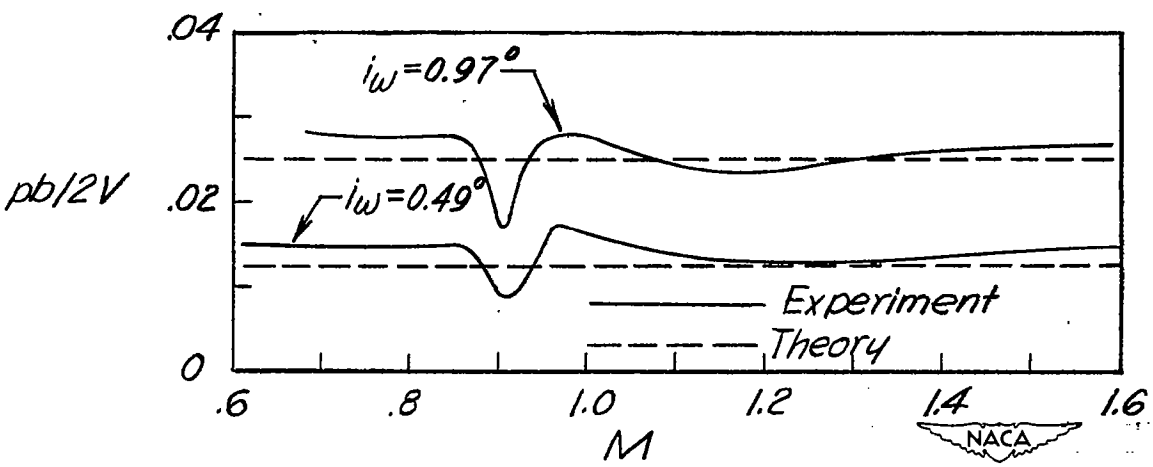

(b) $\Lambda = 0°$; $\frac{1}{m_{\theta_r}} = 1.7 \times 10^{-4}$.

Figure 5.- Comparison between theoretical and experimental values of pb/2V due to incidence. $\delta_a = 0°$; NACA 65A009 airfoil section.

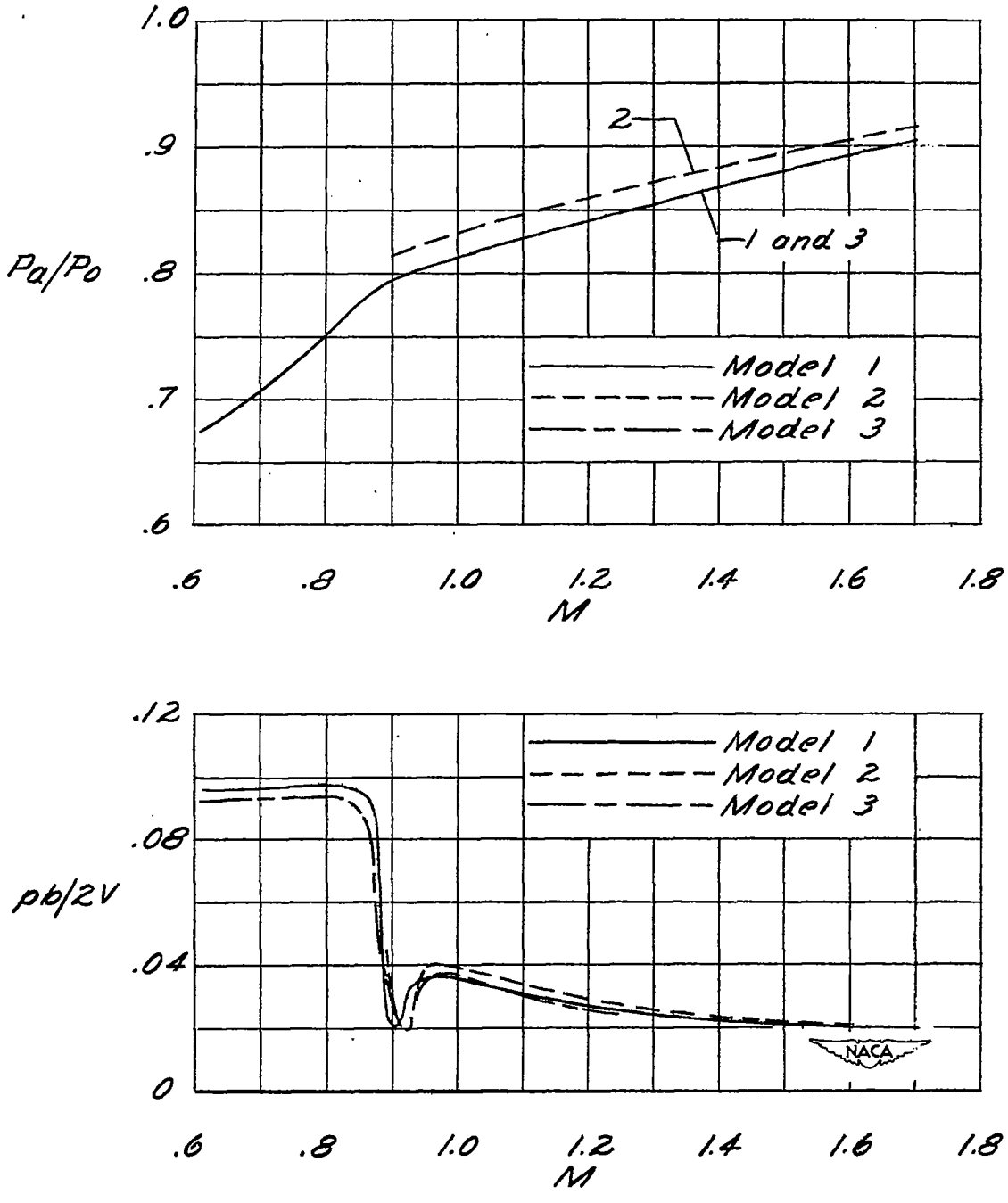

(a) $\frac{1}{m_{\theta_r}} = 1.7 \times 10^{-4}$.

Figure 6.- Variation of pressure ratio and rolling effectiveness with Mach number. $\Lambda = 0^\circ$; $\delta_a = 5.0^\circ$; $i_w = 0^\circ$; NACA 65A009 airfoil section.

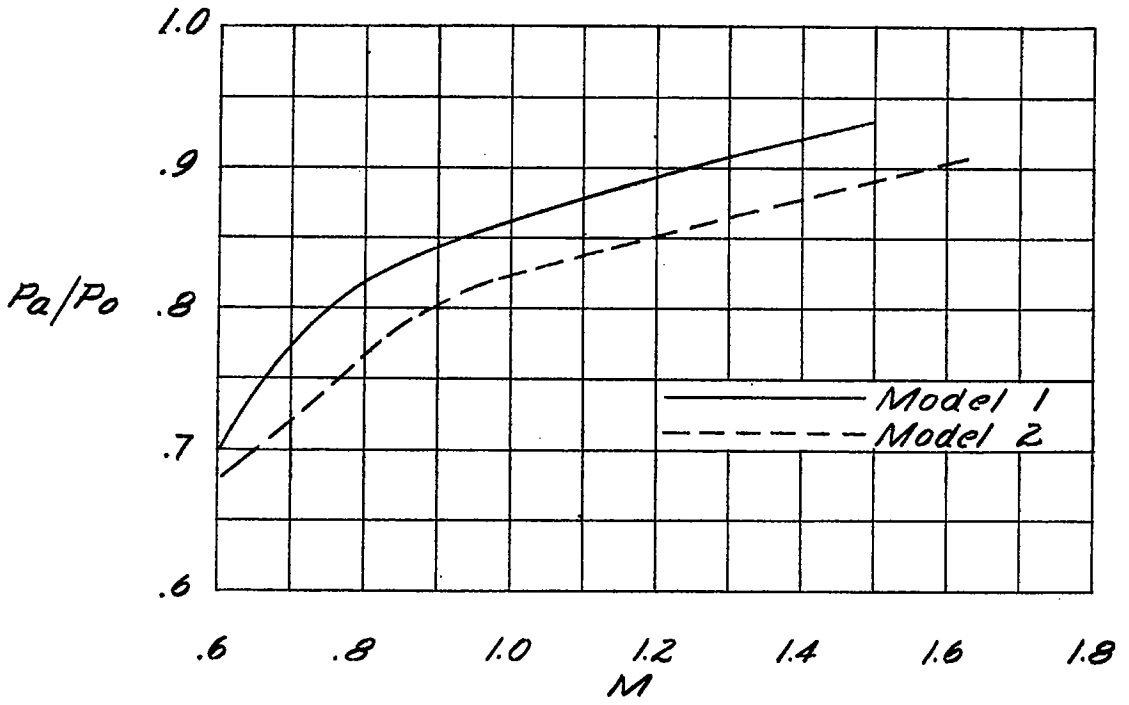

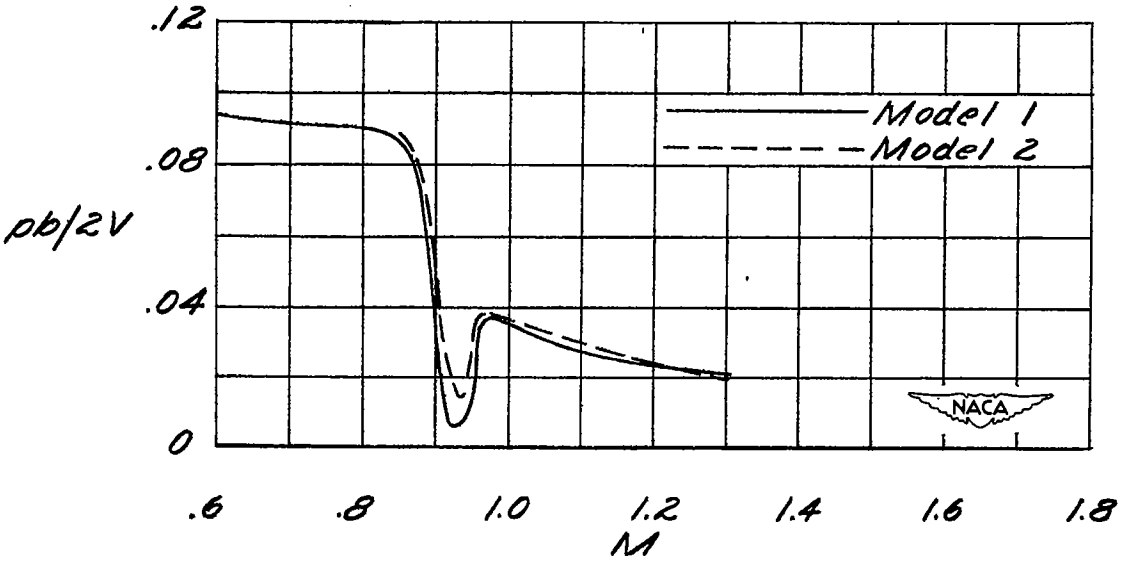

(b) $\frac{l}{m\theta_r} = 2.6 \times 10^{-4}$.

Figure 6.- Continued.

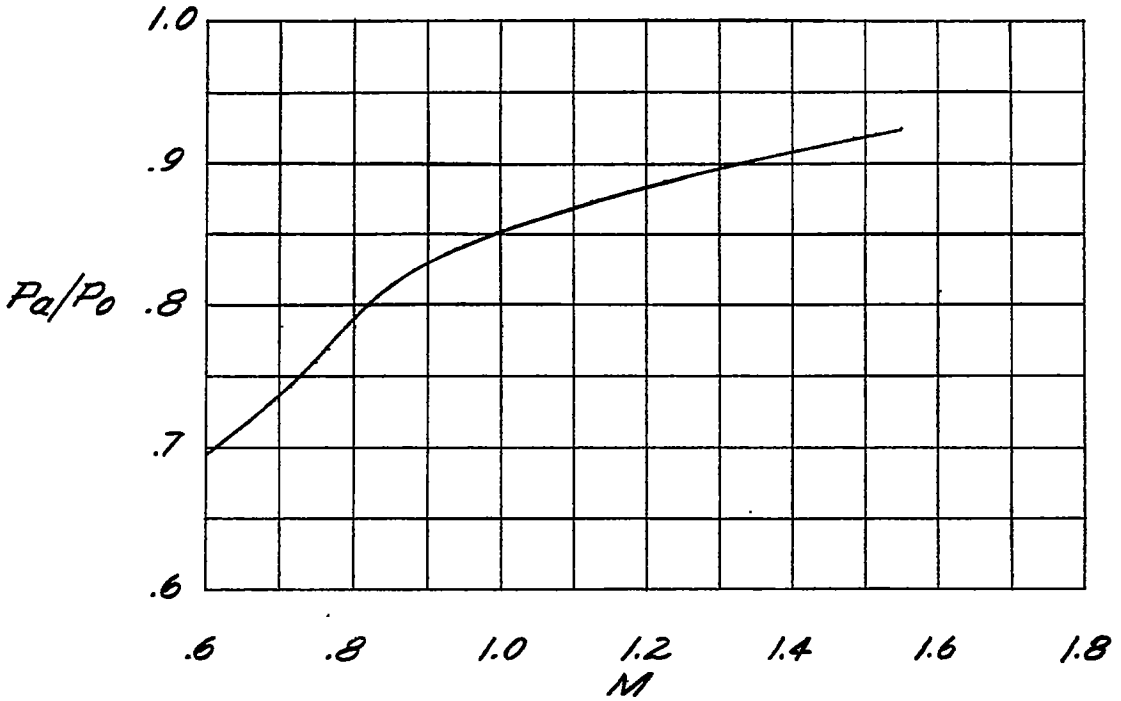

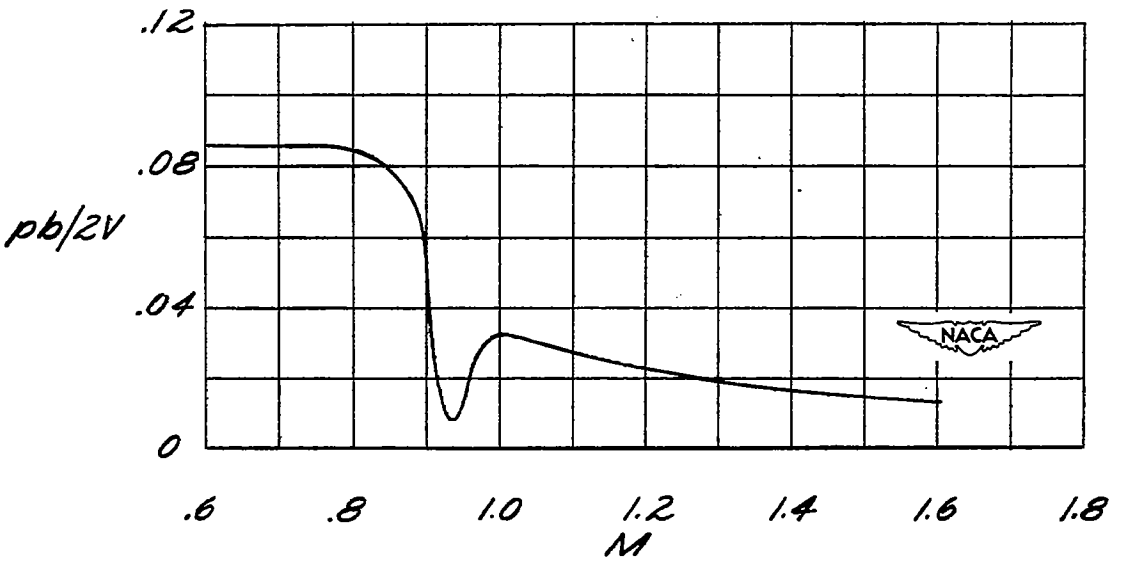

(c) $\frac{l}{m_{\theta_r}} = 4.1 \times 10^{-4}$.

Figure 6.- Continued.

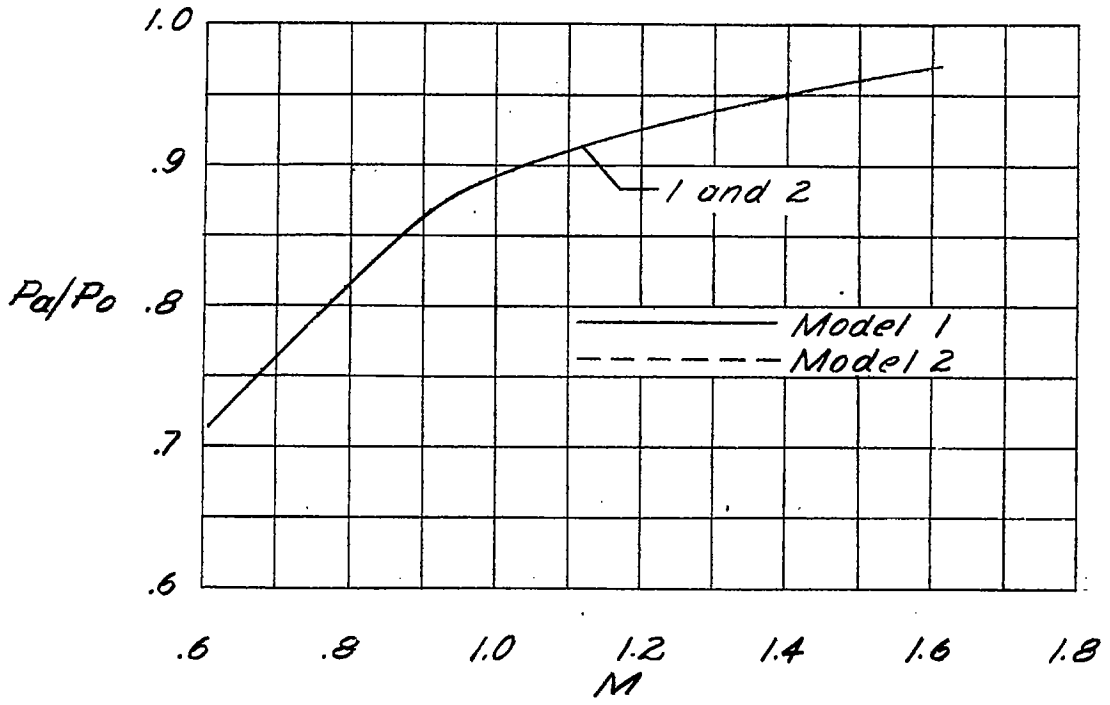

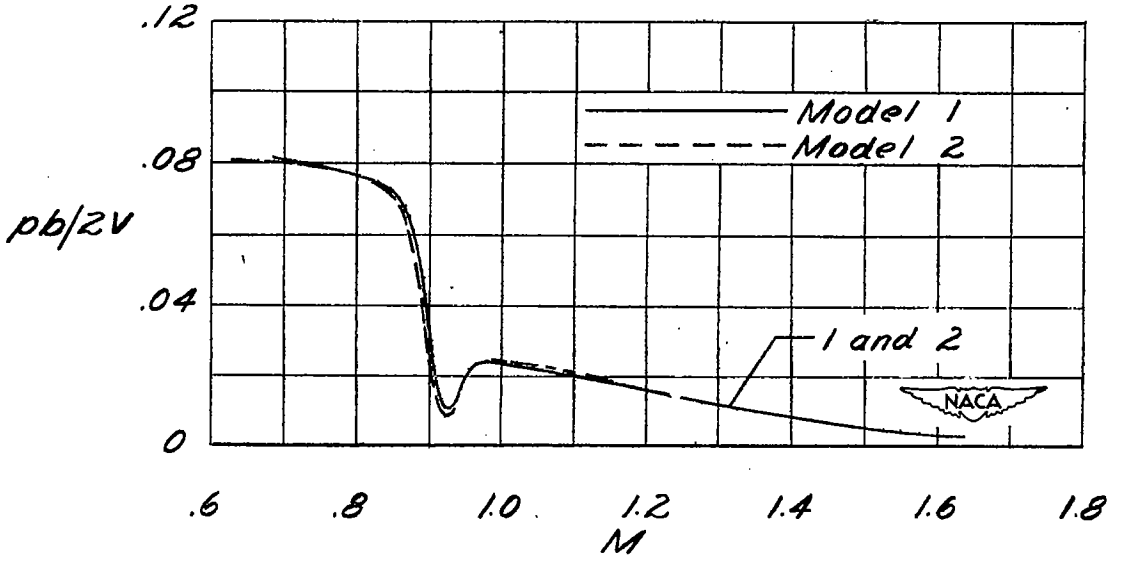

(d) $\frac{1}{m_{\theta_r}} = 9.6 \times 10^{-4}$.

Figure 6.- Continued.

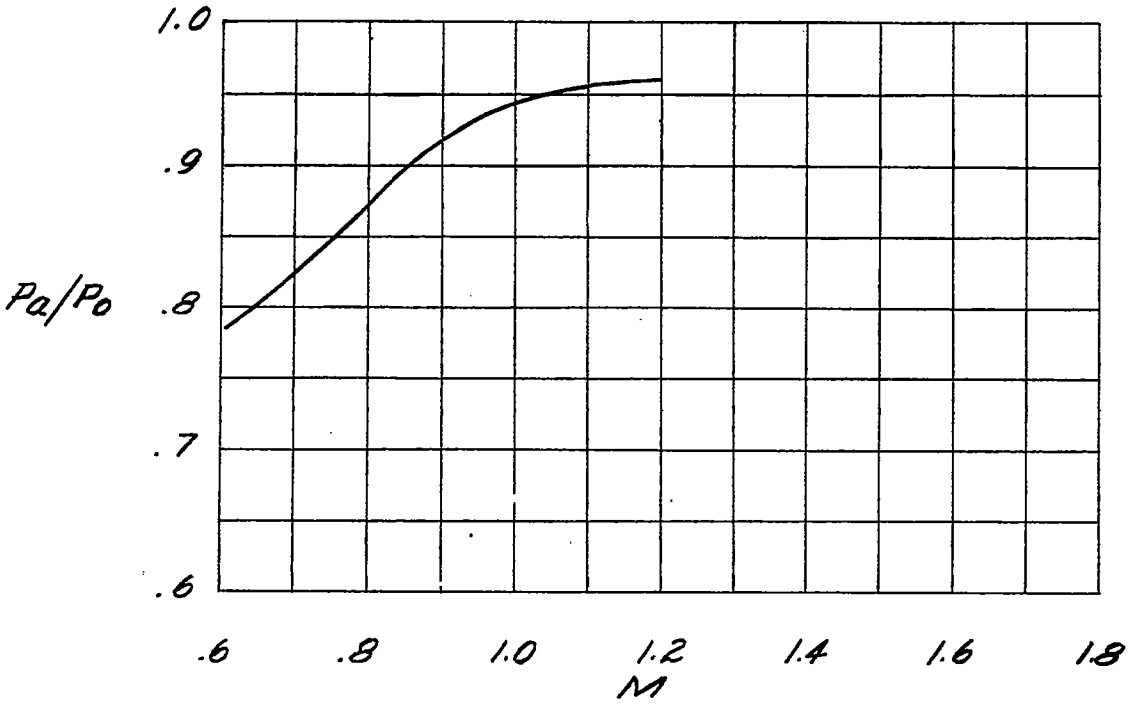

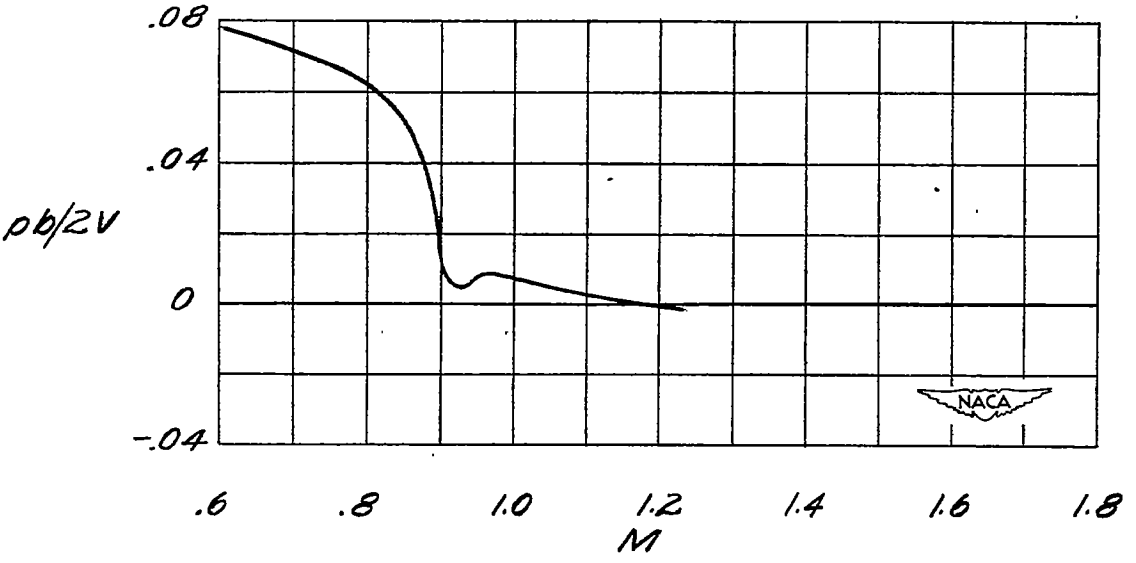

(e) $\frac{1}{m_{\theta_r}} = 15.0 \times 10^{-4}$.

Figure 6.- Continued.

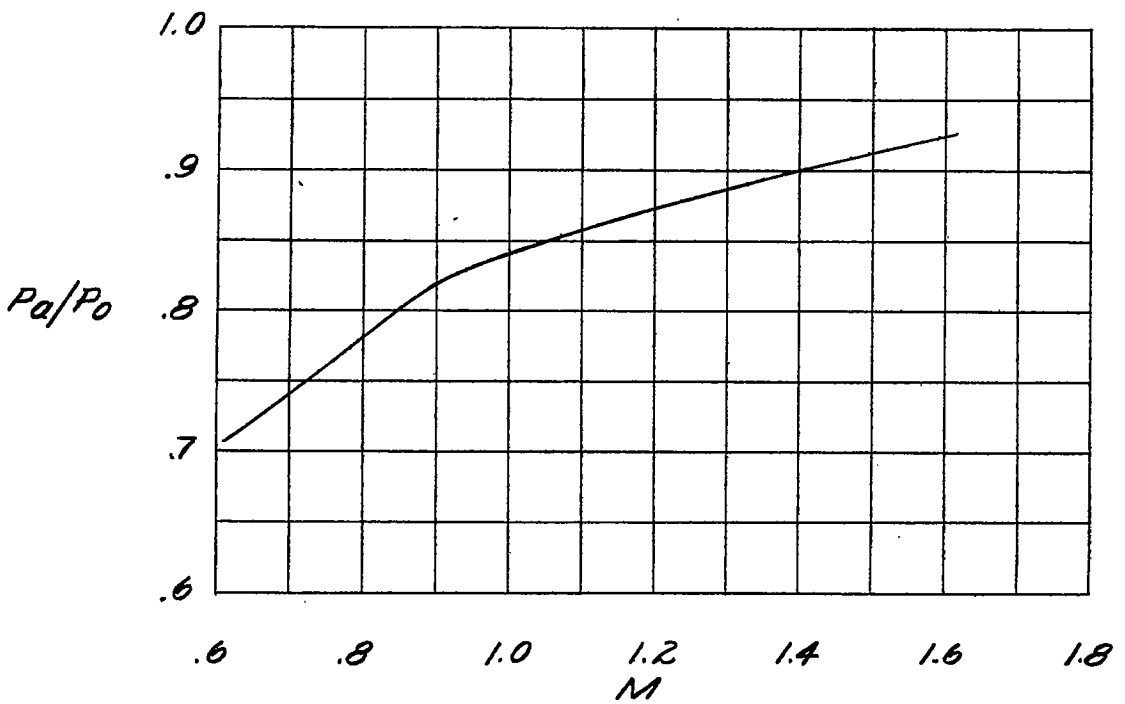

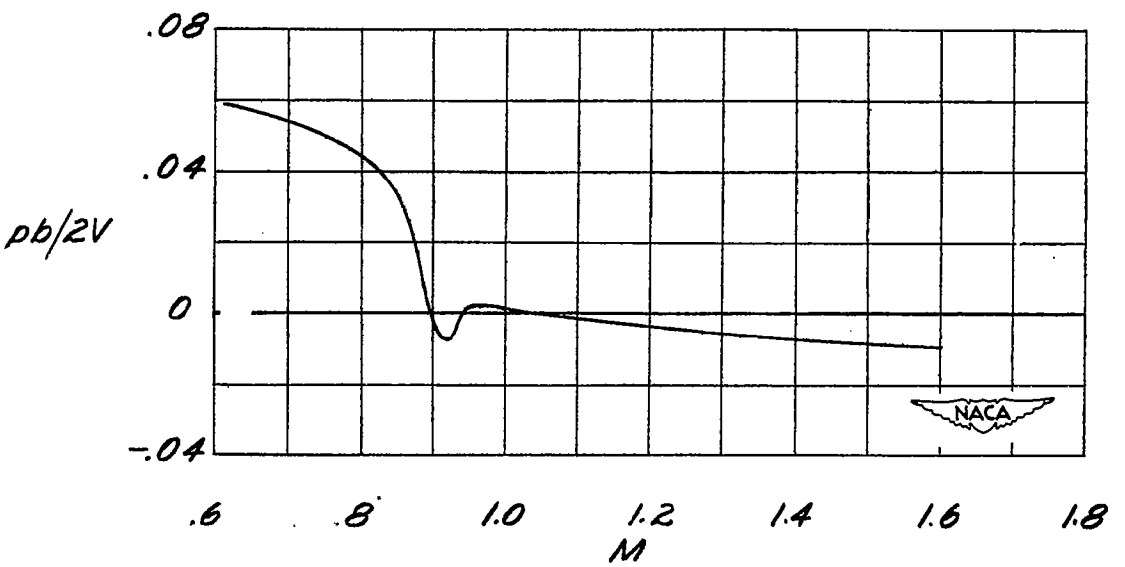

(f) $\frac{l}{m_{\theta_r}} = 15.9 \times 10^{-4}$.

Figure 6.- Concluded.

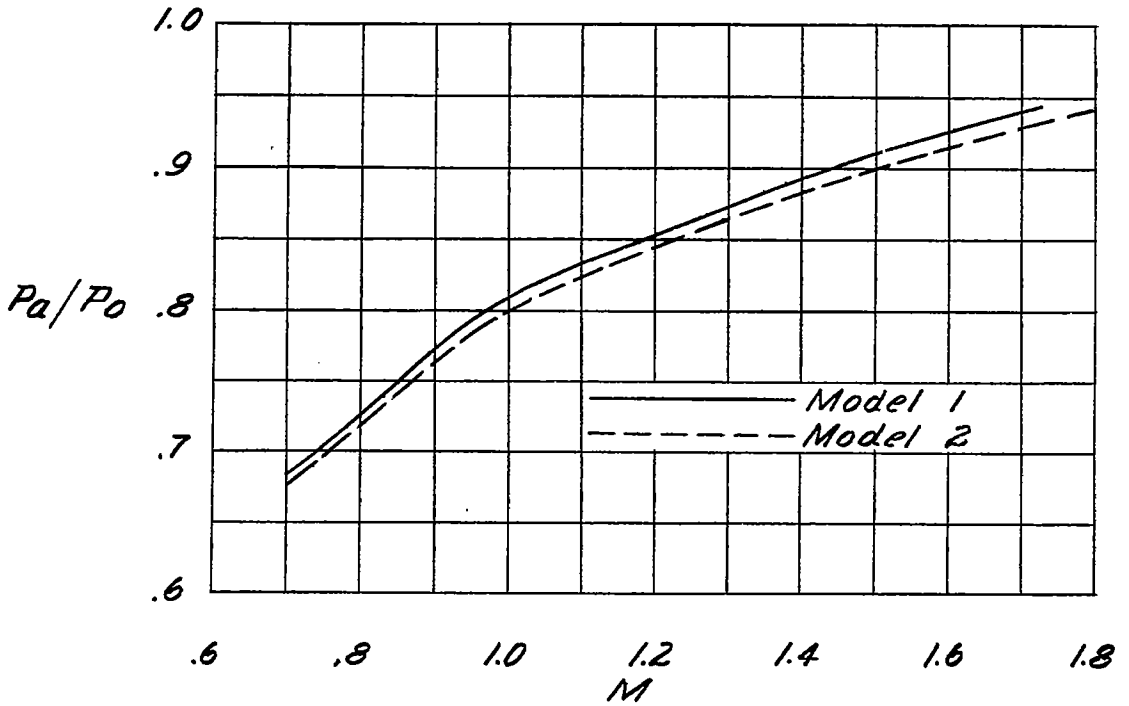

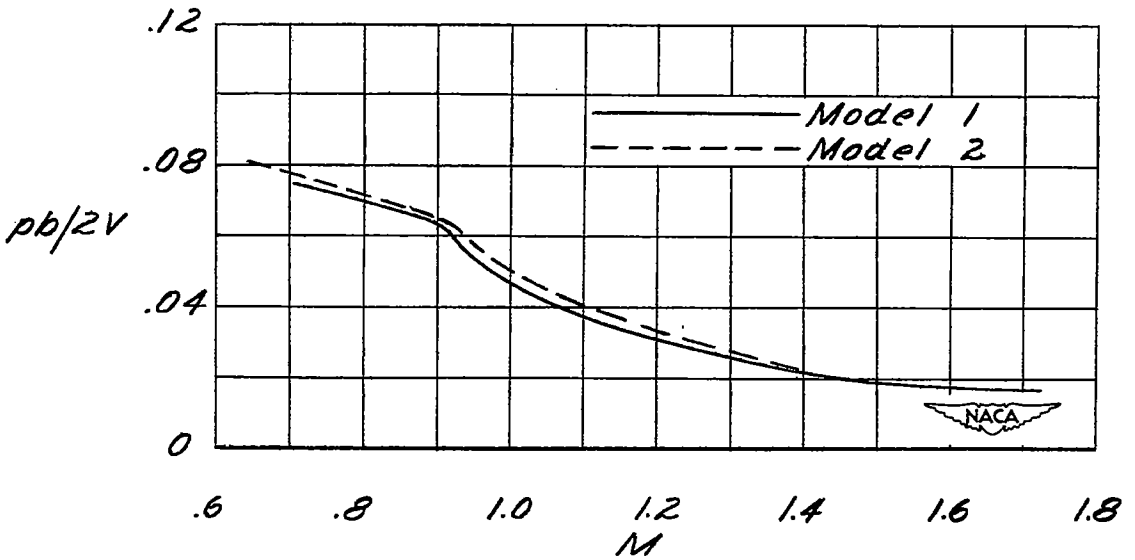

(a) $\frac{l}{m_{\theta_r}} = 3.5 \times 10^{-4}$.

Figure 7.- Variation of pressure ratio and rolling effectiveness with Mach number. $\Lambda = 45^\circ$; $\delta_a = 5.0^\circ$; $i_w = 0^\circ$; NACA 65A009 airfoil section.

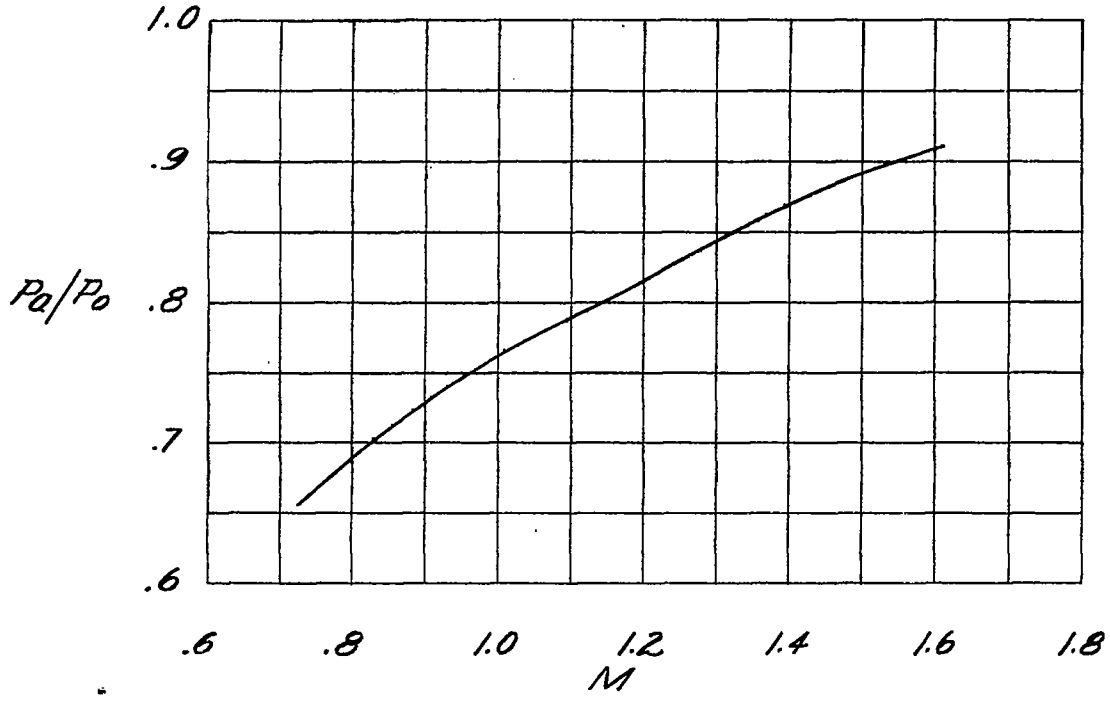

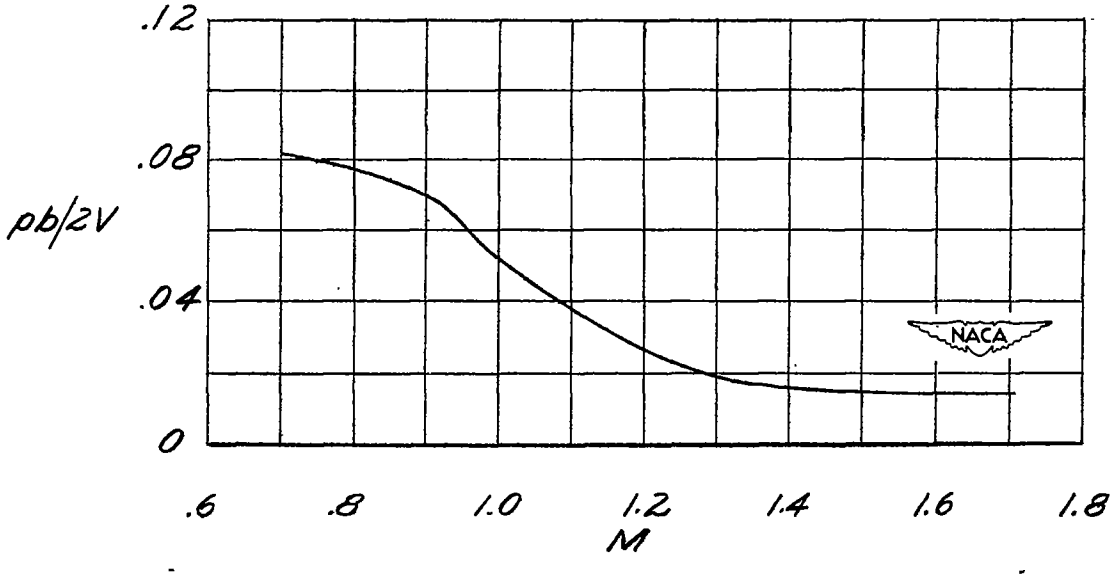

(b) $\frac{1}{m_{\theta_r}} = 4.5 \times 10^{-4}$.

Figure 7.- Continued.

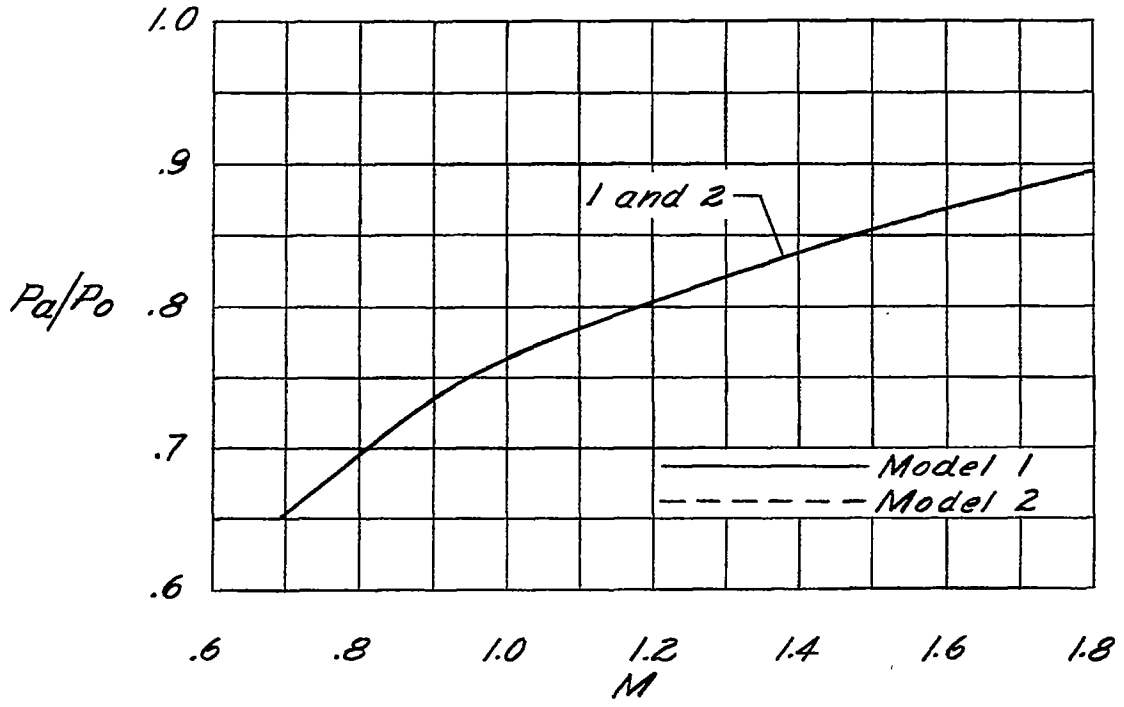

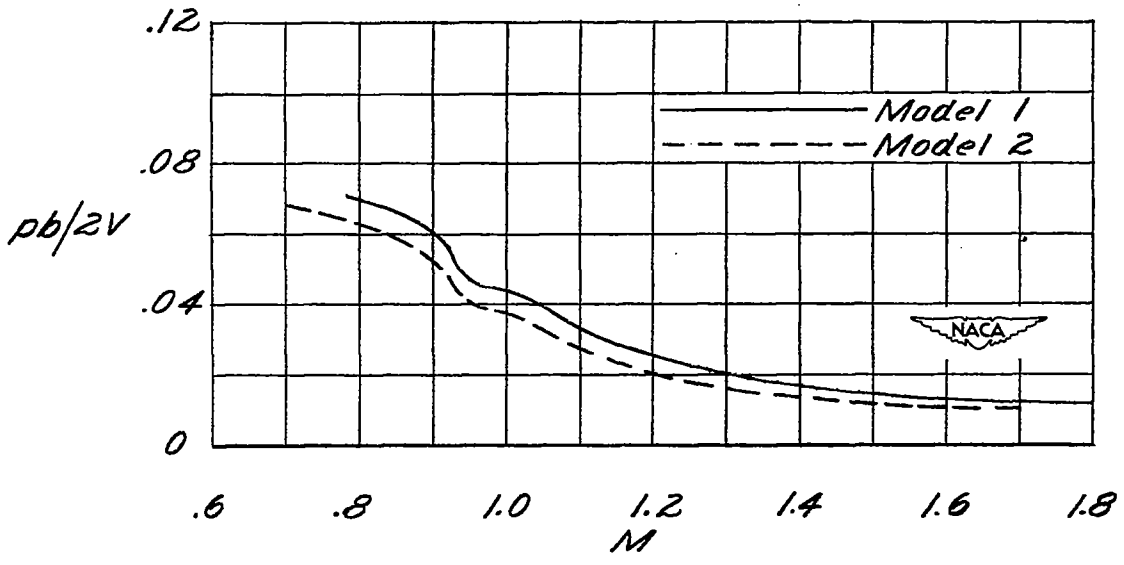

(c) $\frac{1}{m_{\theta_r}} = 6.5 \times 10^{-4}$.

Figure 7.- Continued.

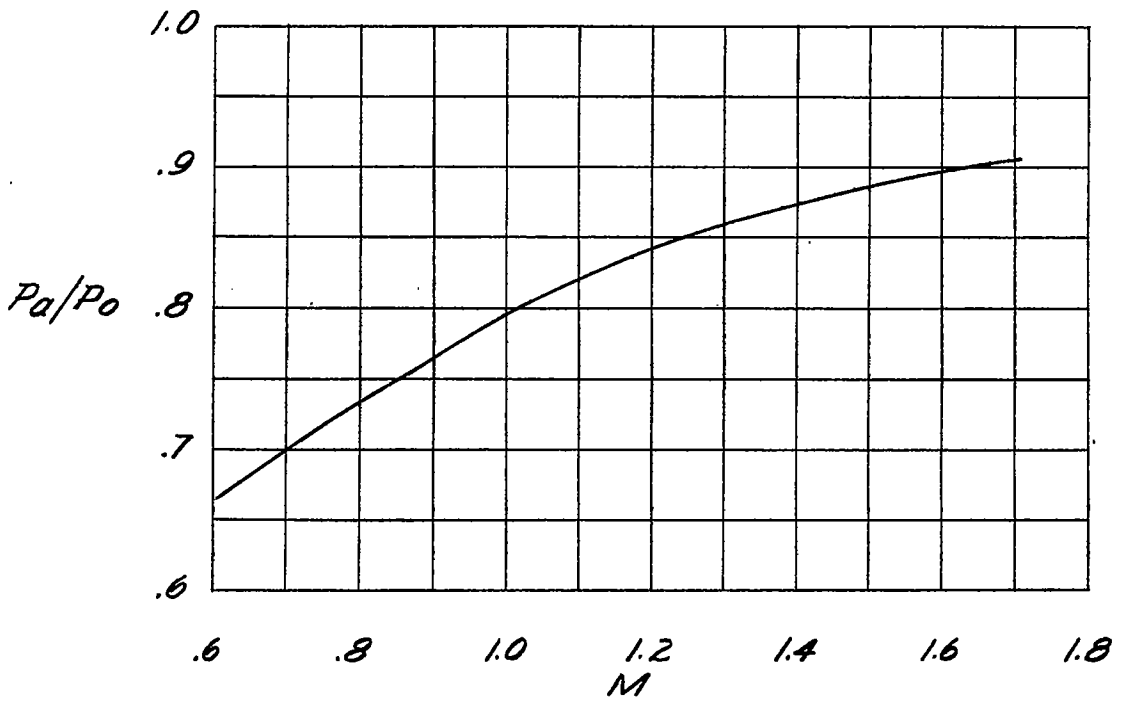

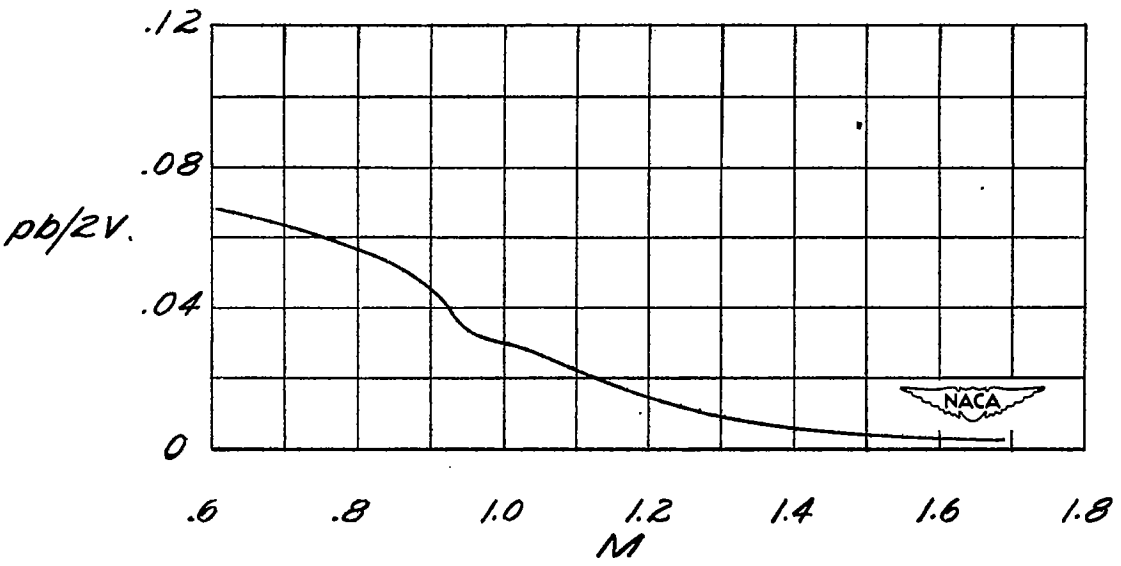

(d) $\frac{1}{m_{\theta_r}} = 12.4 \times 10^{-4}$.

Figure 7.- Continued.

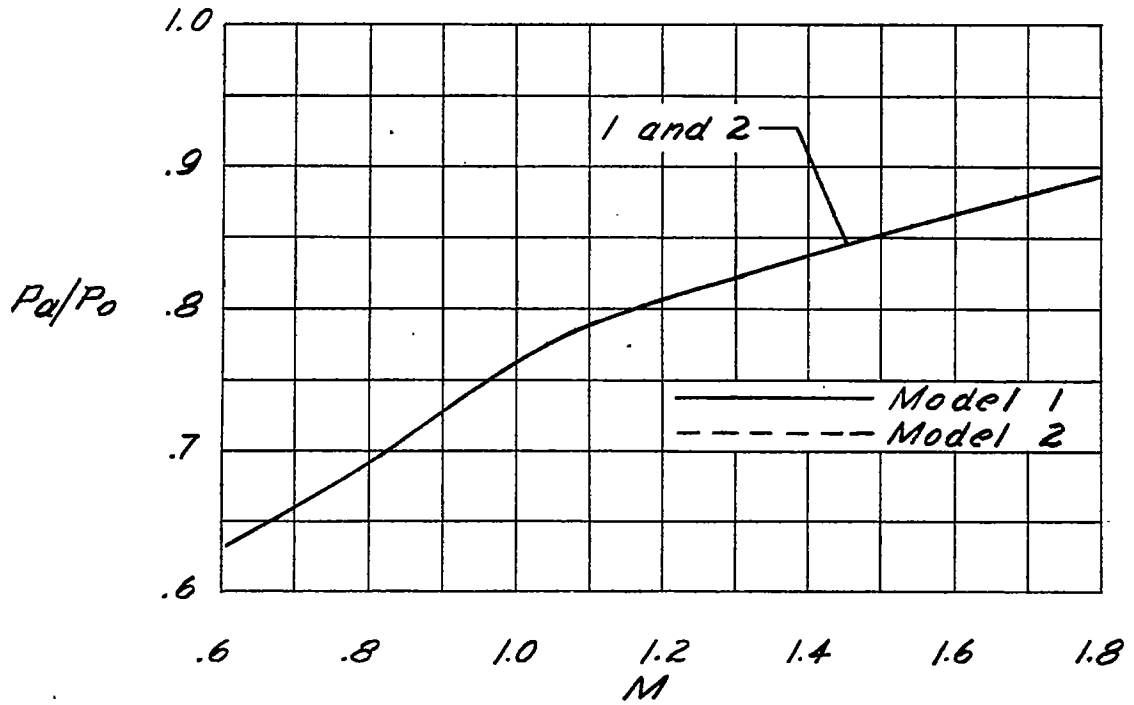

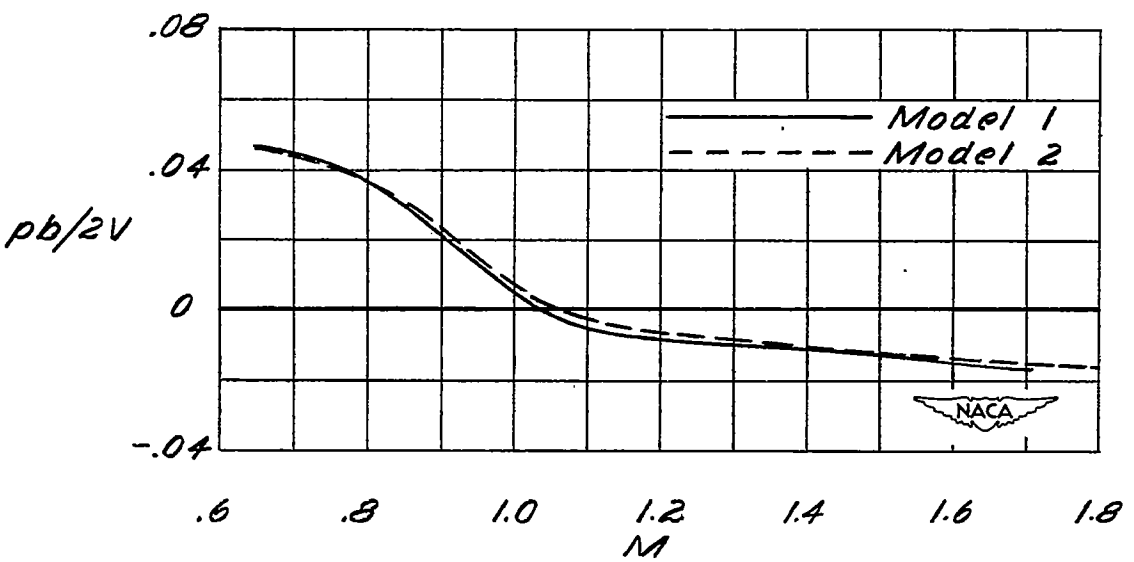

(e) $\frac{1}{m_{\theta_r}} = 23.7 \times 10^{-4}$.

Figure 7.- Concluded.

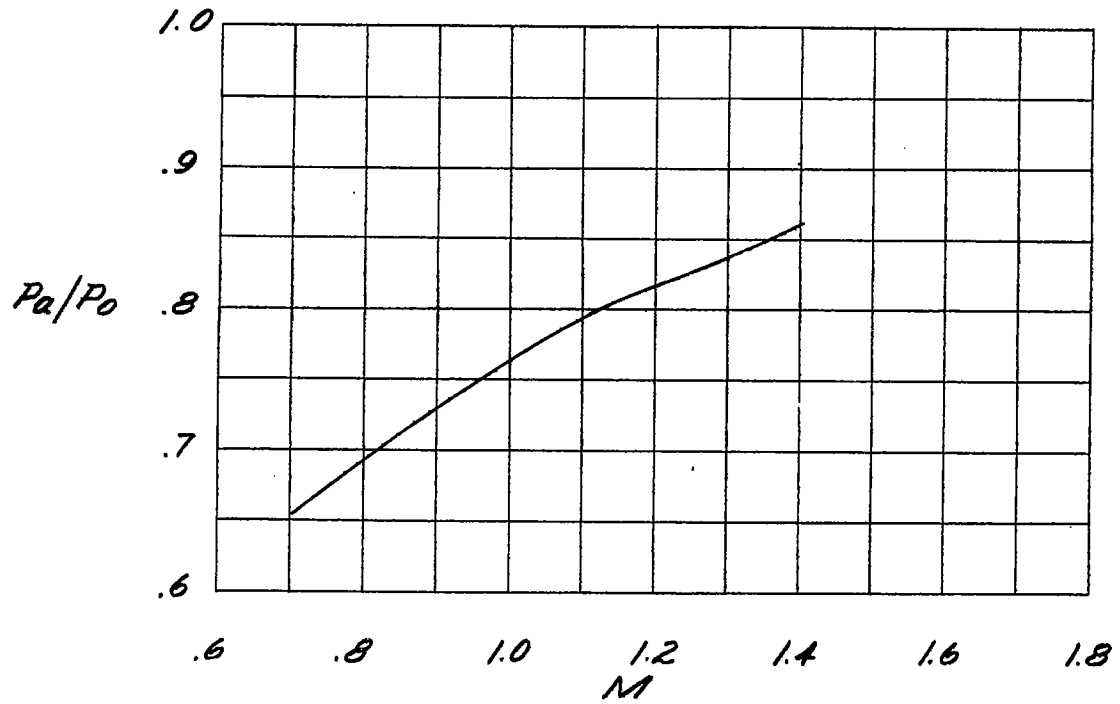

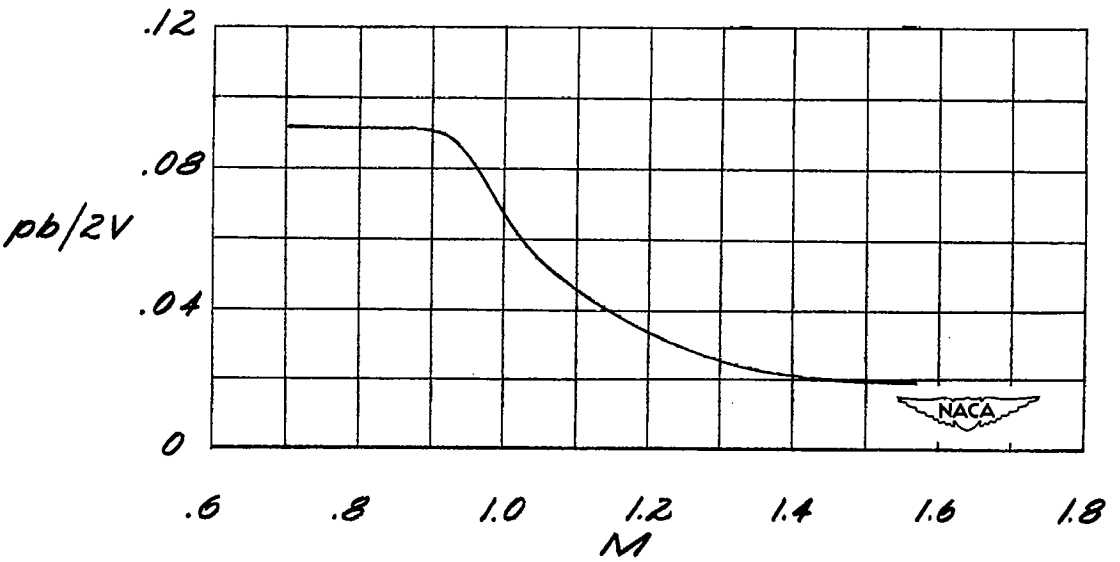

(a) $\frac{1}{m_{\theta_r}} = 4.7 \times 10^{-4}$.

Figure 8.- Variation of pressure ratio, total-drag coefficient, and rolling effectiveness with Mach number. $\Lambda = 0^{\circ}$; $\delta_a = 5.0^{\circ}$; $i_w = 0^{\circ}$; NACA 65A003 airfoil section.

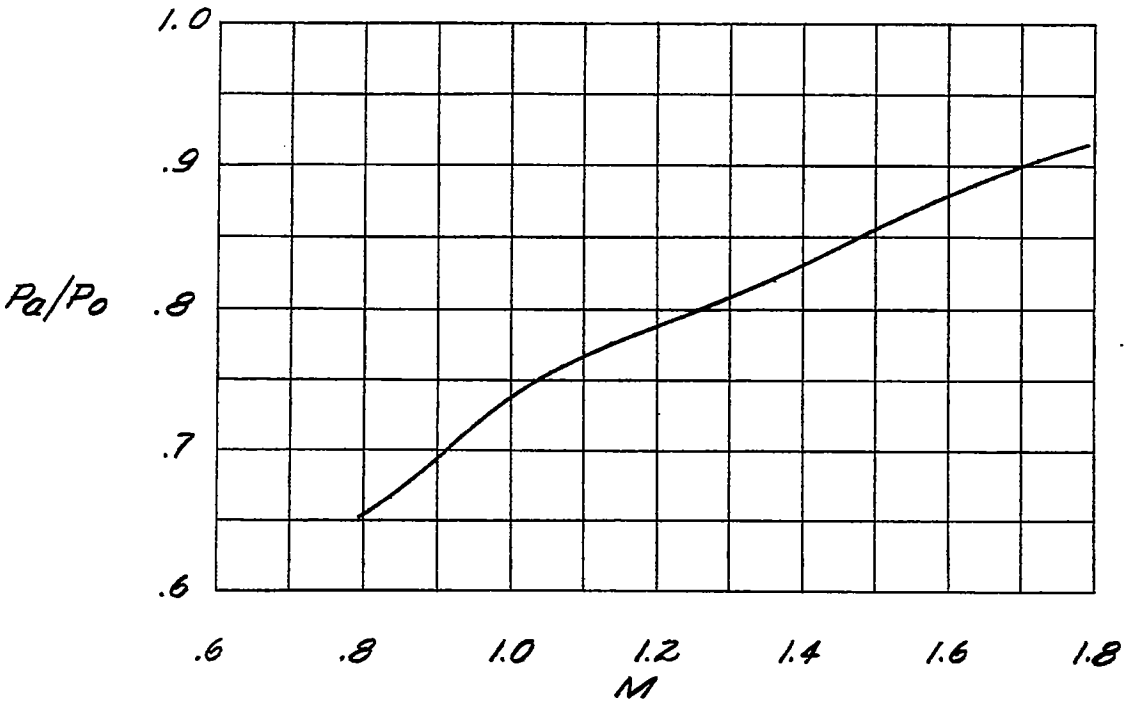

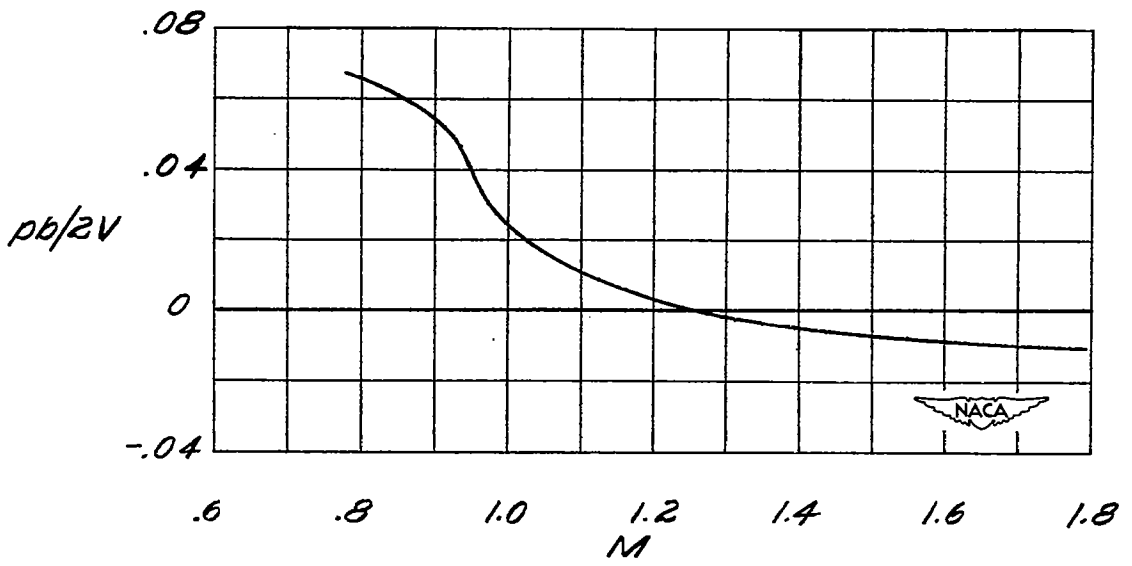

(b) $\frac{1}{m_{\theta_r}} = 14.7 \times 10^{-4}$.

Figure 8.- Concluded.

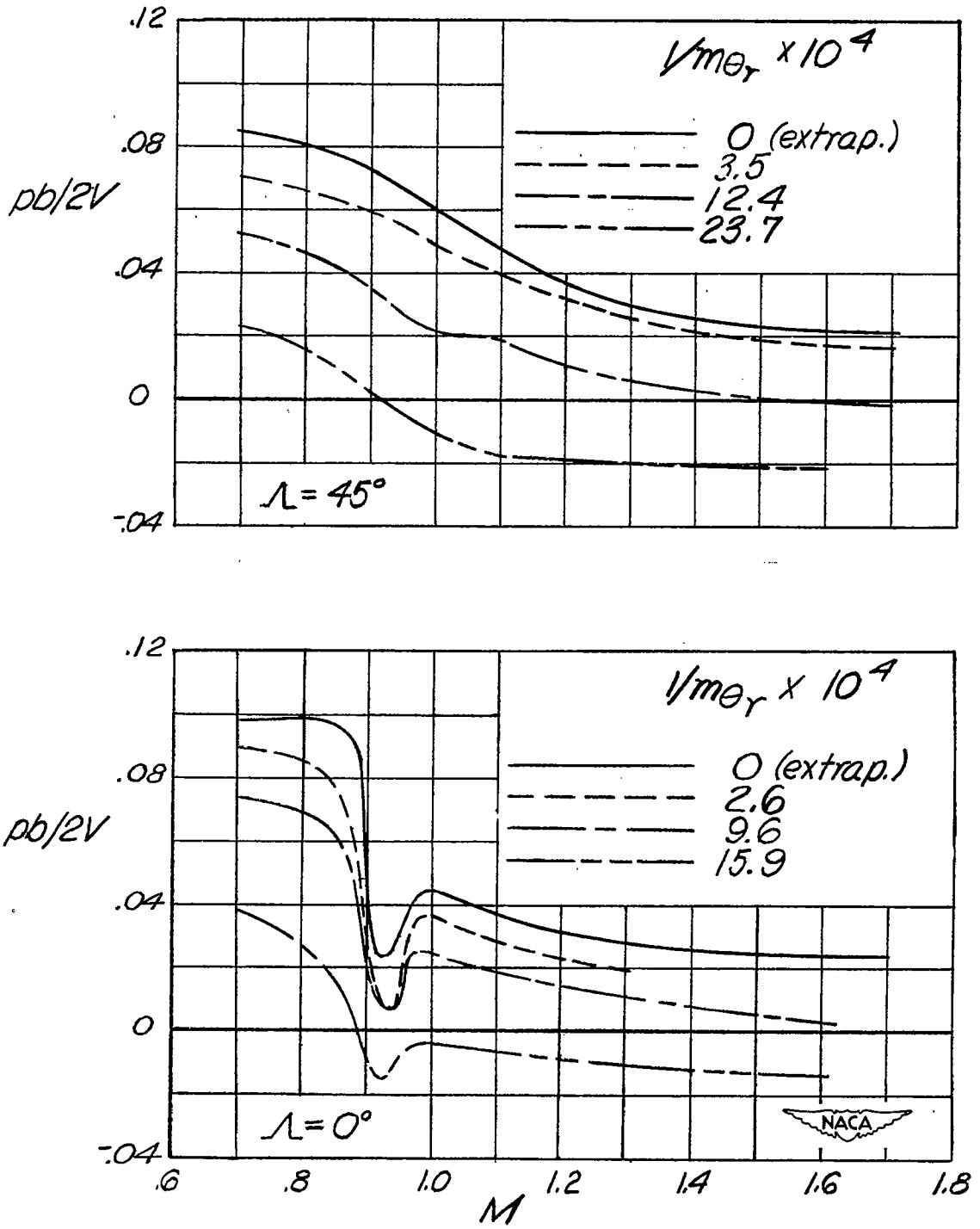

(a) NACA 65A009 airfoil section.

Figure 9.- Effect of decreasing wing torsional rigidity on the variation of rolling effectiveness with Mach number. Corrected to sea-level conditions. $\delta_a = 5.0°$; $i_w = 0°$.

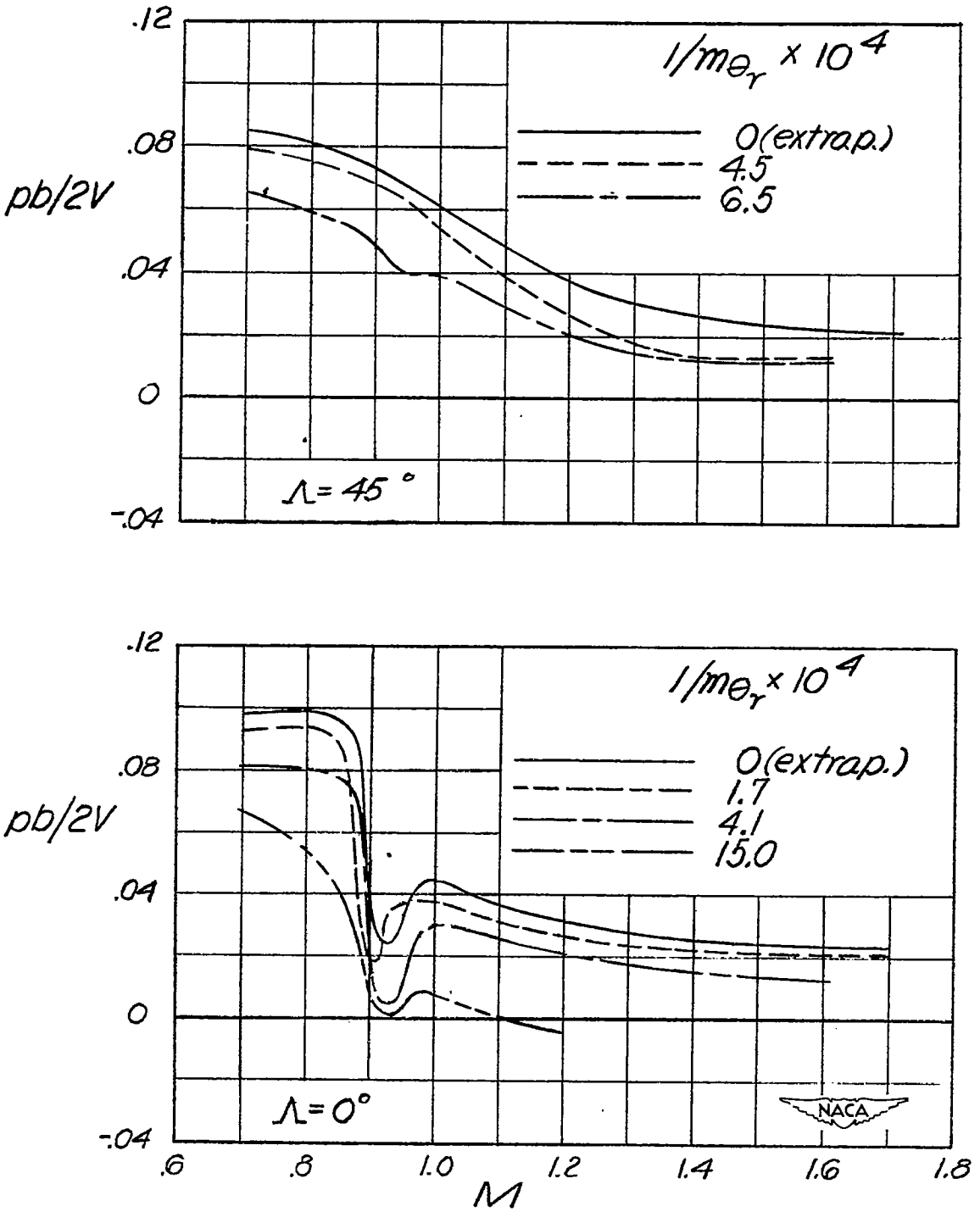

(a) Concluded.

Figure 9.- Continued.

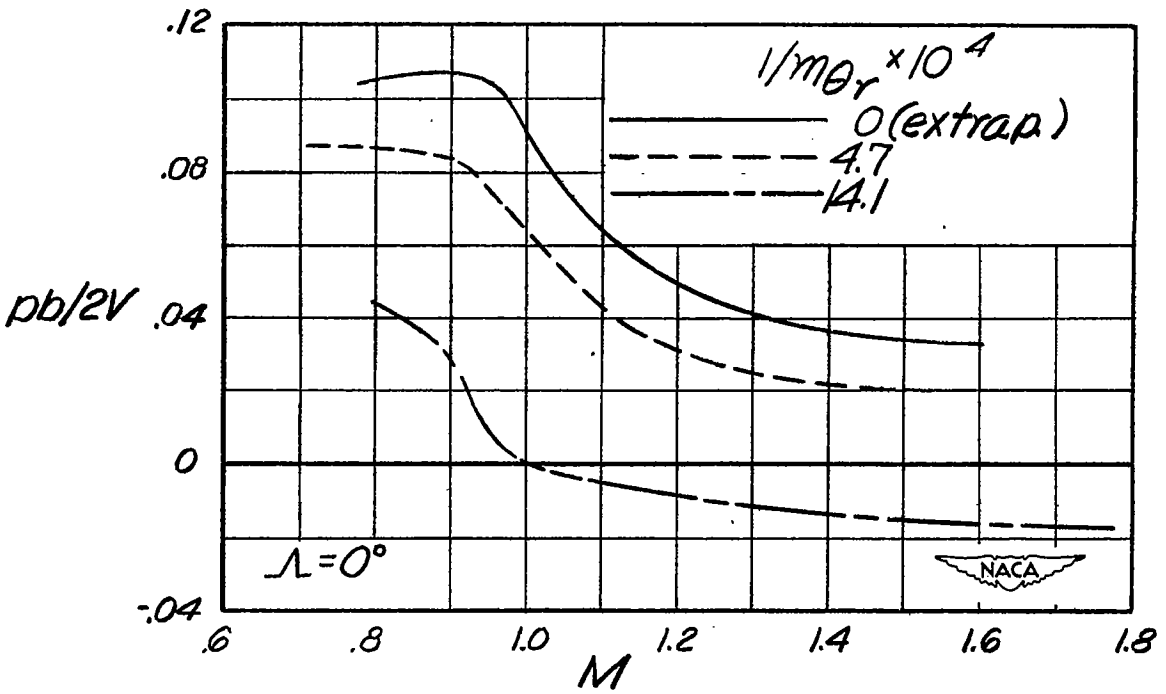

(b) NACA 65A003 airfoil section.

Figure 9.- Concluded.

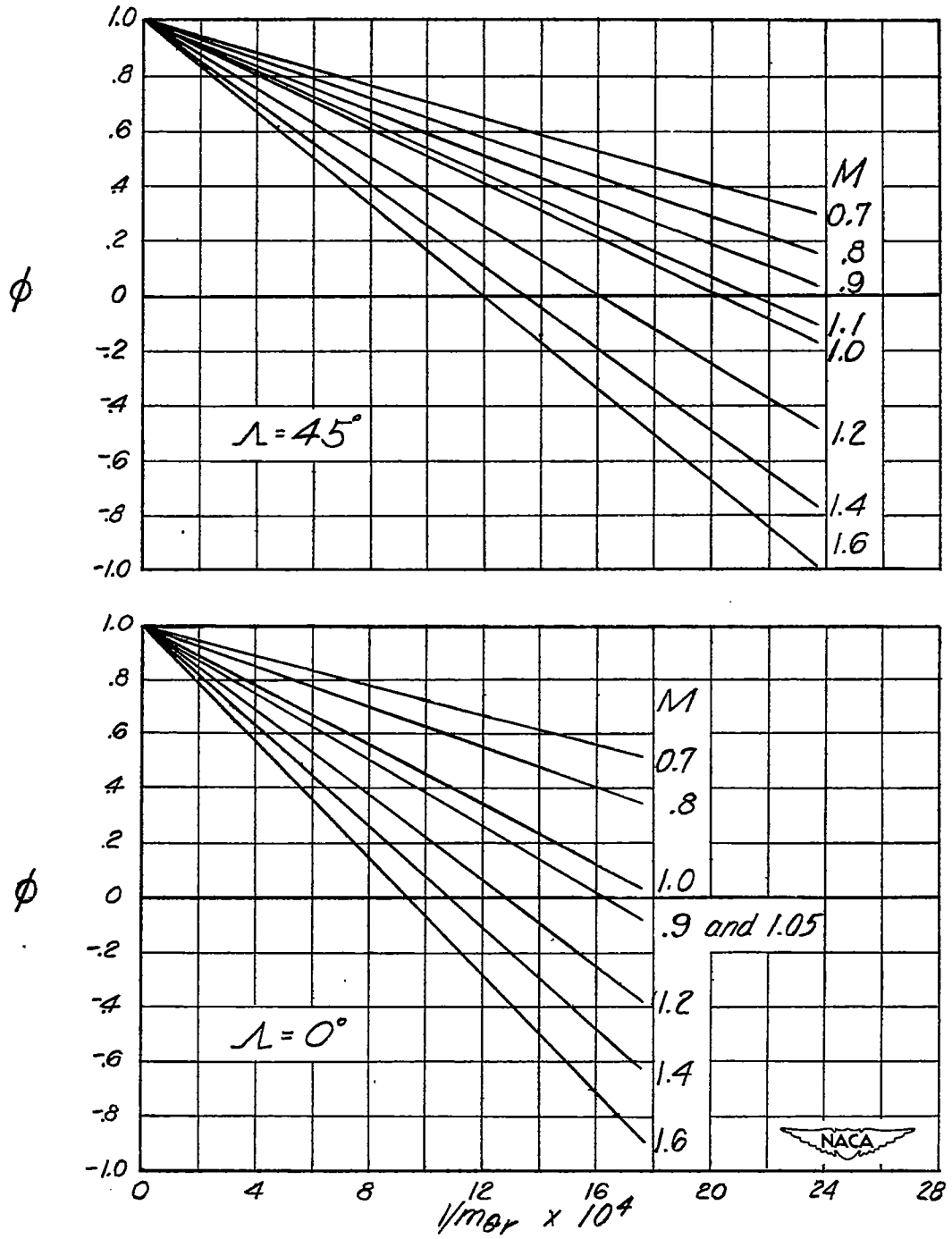

(a) NACA 65A009 airfoil section.

Figure 10.- Effect of increasing Mach number on the variation of the flexible wing-rolling-effectiveness parameter with decreasing wing torsional rigidity. Corrected to sea-level conditions.

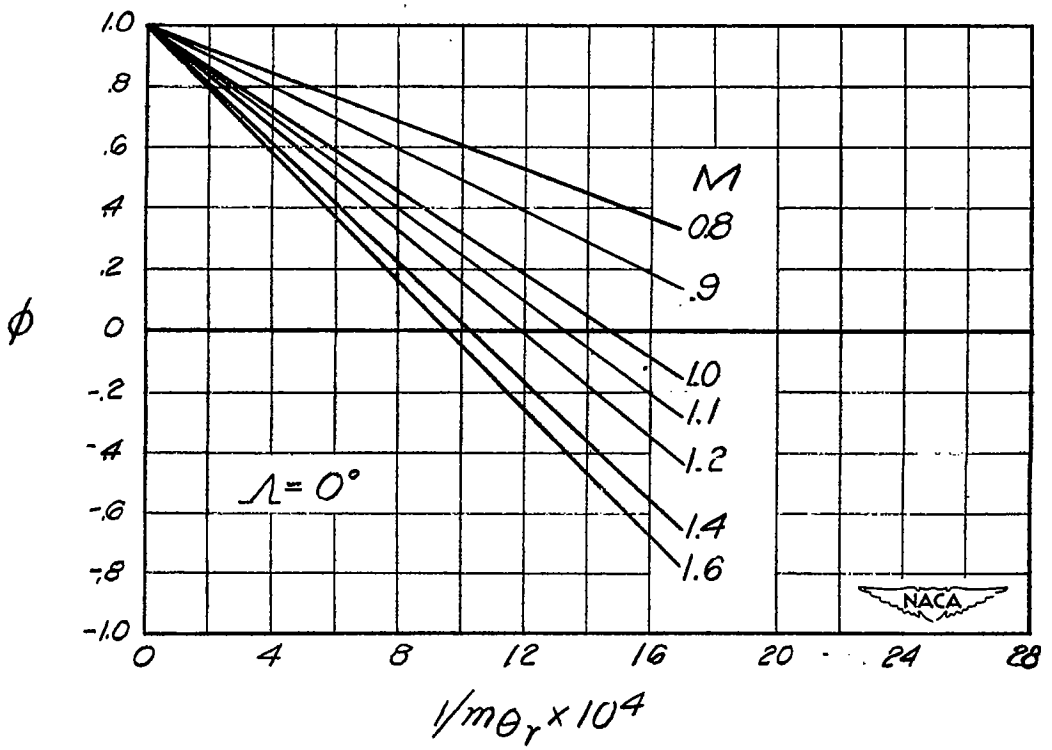

(b) NACA 65A003 airfoil section.

Figure 10.- Concluded.

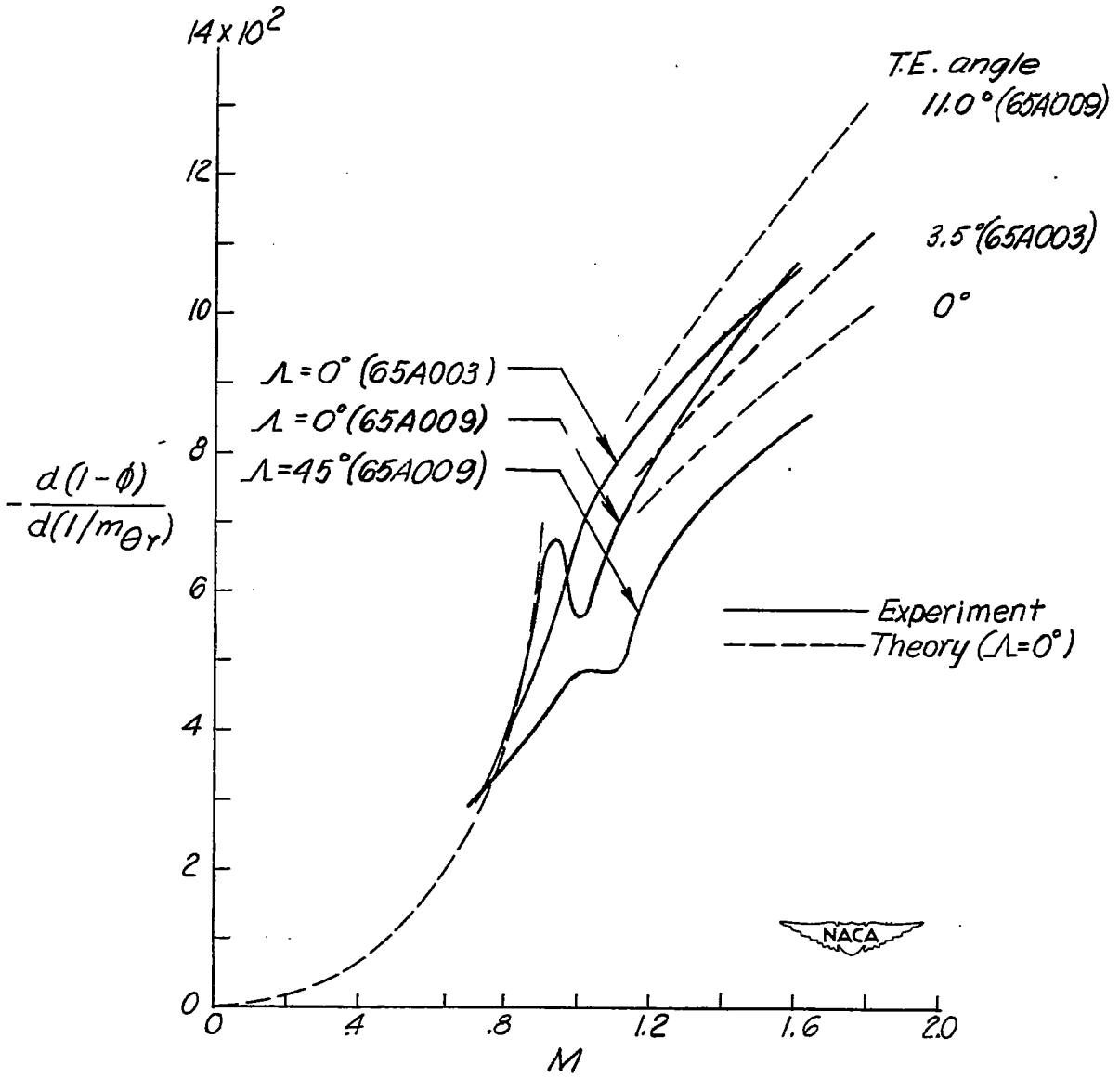

Figure 11.- Comparison between theory and experiment of $-\frac{d(1-\phi)}{d(1/m_{\theta r})}$ as a function of Mach number. Corrected to sea-level conditions.

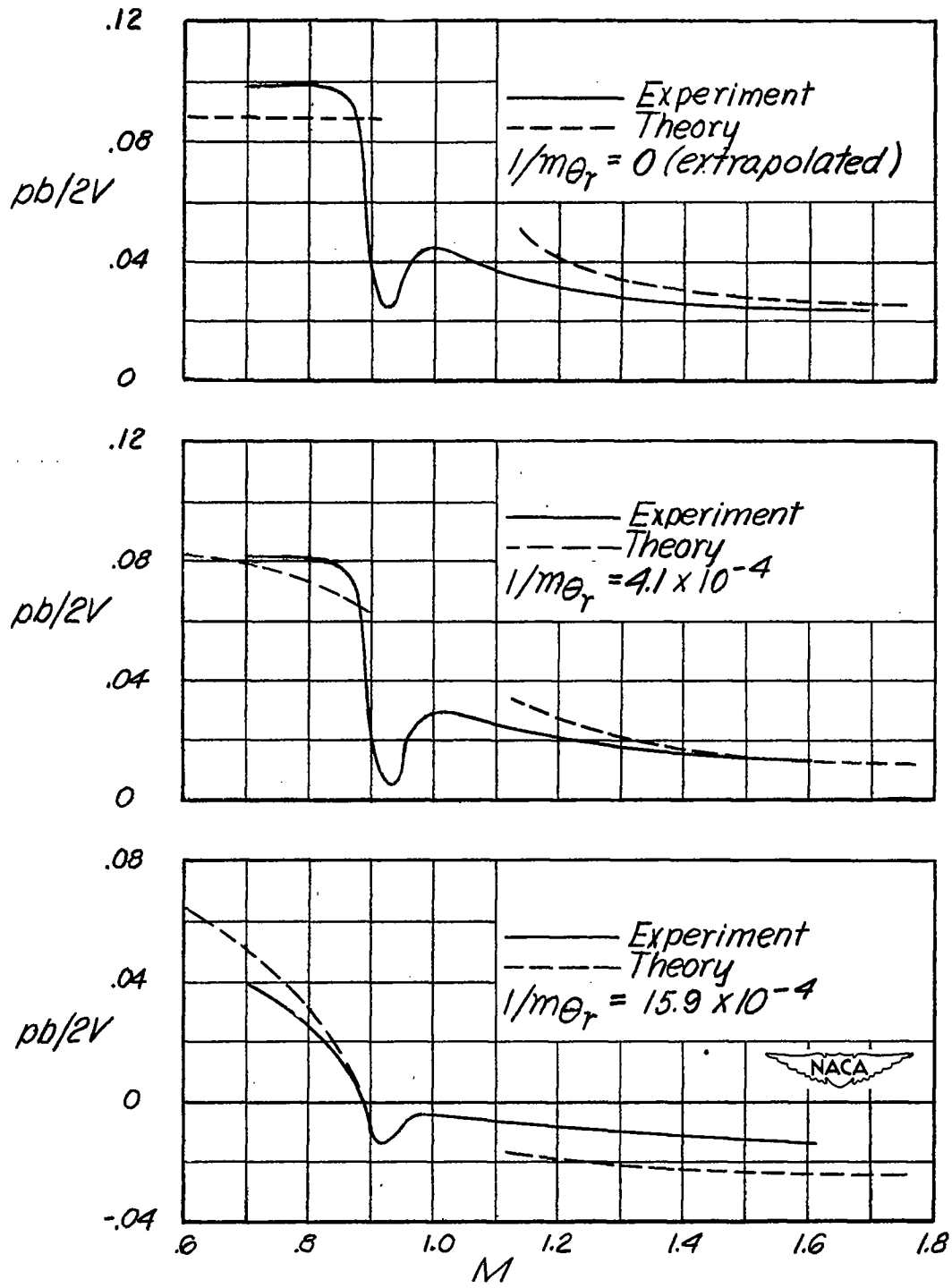

Figure 12.- Comparison between theory and experiment of pb/2V as a function of Mach number. $\Lambda = 0^\circ$; $\delta_a = -5.0^\circ$; $i_w = 0^\circ$; NACA 65A009 airfoil section. Corrected to sea-level conditions.

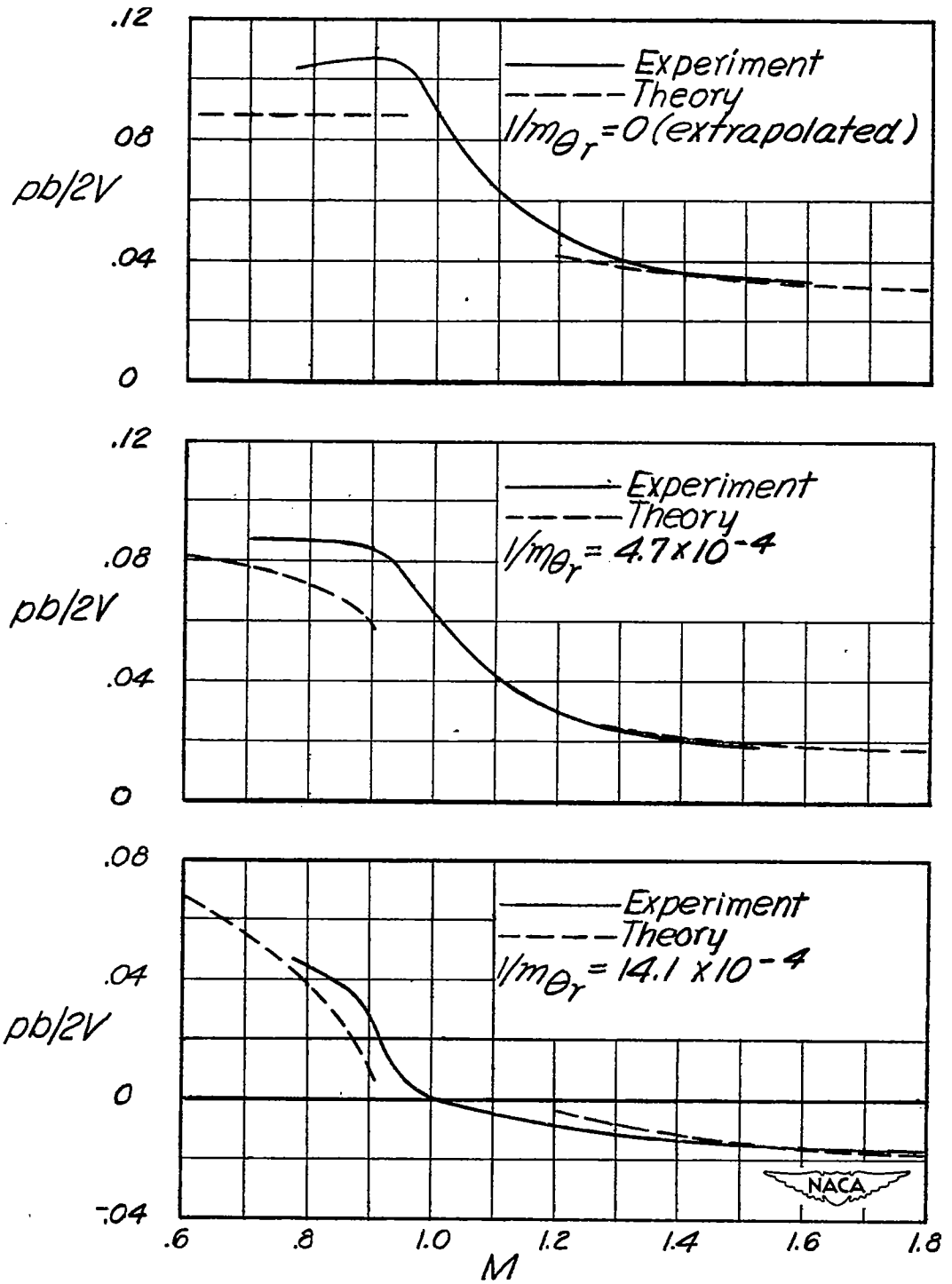

Figure 13.- Comparison between theory and experiment of pb/2V as a function of Mach number. $\Lambda = 0^\circ$; $\delta_a = 5.0^\circ$; $i_w = 0^\circ$; NACA 65A003 airfoil section. Corrected to sea-level conditions.

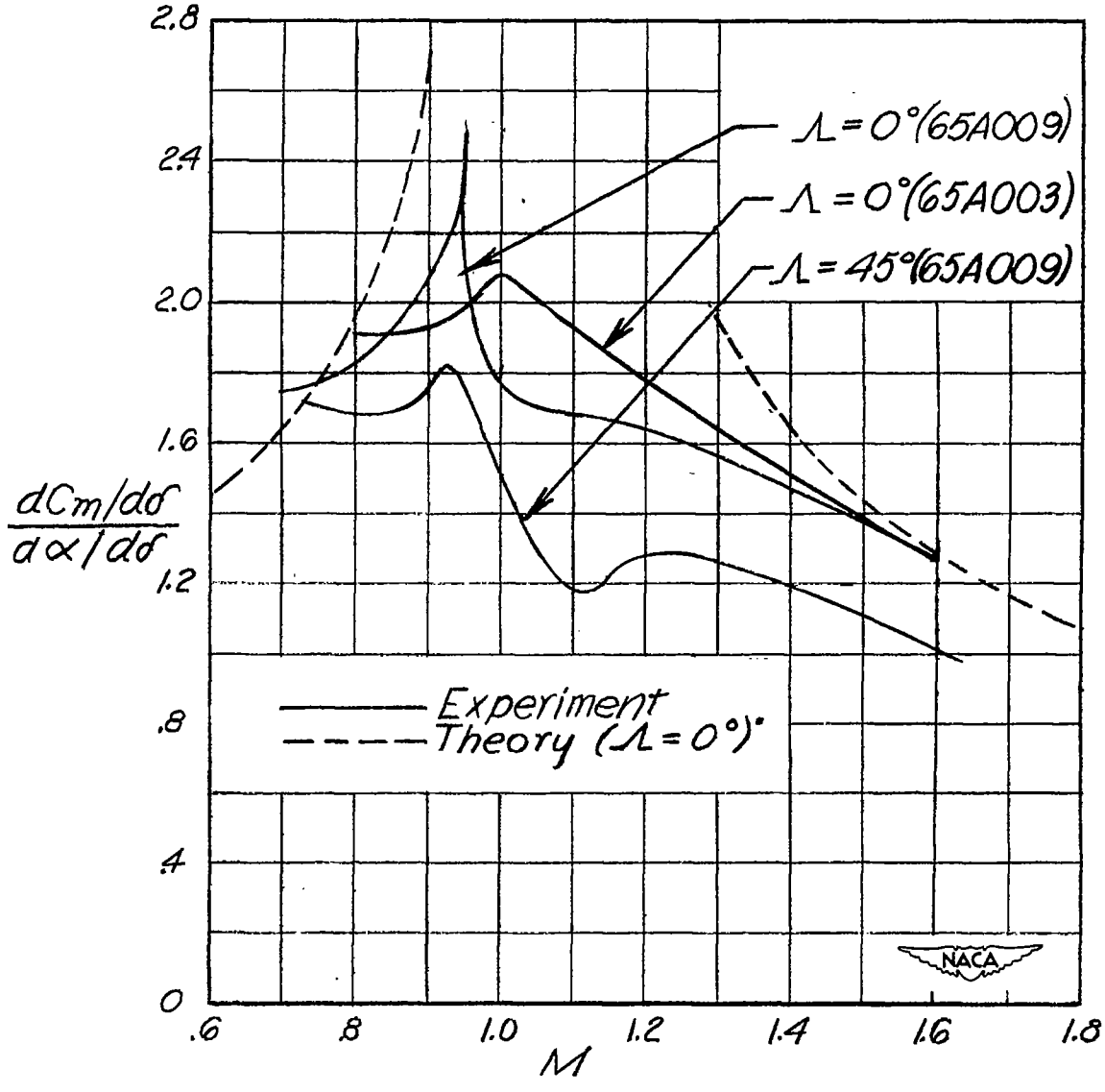

Figure 14.- Variation with Mach number of the effective twisting-moment coefficient evaluated from the experimental rolling-loss data.

NACA-Langley - 10-4-50 - 375